W-AM-Sy1 THE ROLE OF ACTIN IN NON-MUSCLE MOTILE SYSTEMS. L.G. Tilney* (Intr. by D. Caspar) University of Pennsylvania, Philadelphia, Pennsylvania 19174.

Three characteristics of actin in non-muscle cells will be described. First, I will describe the morphological attachment of actin filaments to membranes and whether these filaments attach to intrinsic membrane proteins or not. Second, I will present evidence that demonstrates that much of the actin in non-muscle cells is in a non-filamentous state that can be rapidly transformed into filaments by changing the internal pH of the cell. Third, I will describe how a non-muscle cell may determine the polarity of the actin filaments within it and by doing so control the direction of force production.

W-AM-Sy2 STRUCTURE, FUNCTION AND BIOCHEMISTRY OF INTERMEDIATE (10nm) FILAMENTS. R. Goldman, J. Starger*, A. Goldman, P. Steinert† and E. Wang°, Carnegie-Mellon University, Pittsburgh, Pa.; *MRC Biophysics, London; †National Cancer Institute; °Rockefeller University.

Intermediate-sized filaments (∿10nm diameter) are found in the cytoplasm of many types of cells. In cultured baby hamster kidney (BHK-21) cells, they appear to function in spreading, shape formation, locomotion and, in conjunction with microtubules, in intracellular organelle movement. Juxtanuclear accumulations of 10nm filaments termed filament caps (FC) form following trypsinization and replating of BHK-21 cells. FC are birefringent and a simple technique has been developed for their rapid isolation. The resulting cell-free preparations of FC appear virtually identical to those seen in situ. BHK-21 FC contain masses of 10nm filaments and SDS-PAGE reveals that there are major subunits of ∿54,000 and 55,000 molecular weight. The FC rapidly lose their birefringent properties and the majority of 10nm filaments disassemble in solutions of low ionic strength. Reassembly is achieved by the addition of physiological concentrations of NaCl. Reassembled BHK-21 filaments contain ∿42% α-helix and display a wide angle x-ray diffraction pattern which is very similar to keratin. In addition, the overall morphology, dimensions and amino acid composition of BHK-21 10nm filaments are similar to keratin filaments. FC have also been isolated from cultures of chick embryo, rat kangaroo, mouse fibroblast, human skin fibroblast and mouse neuroblastoma cells. In each preparation there is a major subunit of ∿55,000 molecular weight. When these subunits are further analyzed by one-dimensional peptide mapping following limited proteolysis, a great deal of homology is seen amongst them. Based on these observations, we have decided to name this apparently common subunit, decamin. (Supported by the NSF and NCI.)

W-AM-Sy3 PARTICIPATION OF CYTOPLASMIC CONTRACTILE PROTEINS IN CELLULAR STRUCTURE AND MOTILITY. Thomas D. Pollard. Department of Cell Biology and Anatomy, The Johns Hopkins Medical School, Baltimore, Md.

I will review the properties of the cytoplasmic actins and myosins with emphasis on the features that distinquish these contractile proteins from their counterparts in muscles. The myosins from the non-muscle cells are particularly variable from species to species and at least one cell, Acanthamoeba, has several different types of myosin molecules each with distinctive properties. The actins vary little from each other. For example, even Acanthamoeba and rabbit muscle actins have nearly identical primary structures and all actins form similar filaments. These cytoplasmic contractile proteins have been associated with two cellular functions: force generation for cell motility and maintenance of cytoplasmic structure by virtue of their ability to form a high viscosity gel. The evidence for their role in cell motility includes the similarity of their biochemical properties to those of muscle contractile proteins, their ability to form contractile gels and threads, and their localization at sites of movement such as the cytokinetic contractile ring. Recent evidence for actin-microtubule interactions suggests that the contractile proteins may even power some microtubule-dependent movements. Cells contain a variety of protein molecules which can cross-link actin filaments to form a gel. It is believed that such cross-linked actin filament gels are responsible for the high consistency of the cytoplasm. Both gel formation and contraction are regulated (at least in part) by the Ca^{++}concentration. Micromolar concentrations of Ca^{++} stimulate contraction and inhibit gel formation. The molecular basis of this Ca^{++} regulation is not yet completely understood. In the case of contraction, the regulation involves the phosphorylation of either the myosin heavy chain or light chain which activates the actin-myosin ATPase.

W-AM-Sy4 MICROTUBULES, CELL SHAPE, AND MORPHOGENESIS

B. Burnside, University of California, Berkeley, Department of Physiology-Anatomy, Berkeley, California, 94720.

Embryonic morphogenetic processes are often corellated with programmed changes in cell shape. In fact, in some cases it can be shown that cell shape changes provide the motive force for morphogenetic movement. Though this correlation is an old tenet of embryology, we have known little about the cellular mechanism responsible for achieving cell shape change. We have known even less about the supracellular mechanism responsible for the temporal and spacial programing of individual cell shape changes into the elegantly coordinated movements of morphogenesis. Now, however recent advances in our understanding of motility make it interesting to re-examine the old problem of cell shape in morphogenesis. Using vertebrate neurulation as a model for discussion, we will examine possible mechanisms of cell shape determination and then speculate on how these cell shape changes might be coordinated to produce morphogenetic movement.

W-AM-A1 ^{17}O NMR RELAXATION IN CARBONIC ANHYDRASE SOLUTIONS. K.D. Rose* and R.G. Bryant, Department of Chemistry, University of Minnesota, Minneapolis, MN 55455.

NMR relaxation measurements have been made in an attempt to study the water molecule or molecules directly associated with the metal in the active site of various metallocarbonic anhydrase derivatives. The ^{17}O NMR relaxation data, with and without ^{1}H decoupling, show that the dominant contribution to the NMR relaxation in the enzyme solution, whether the metal in the active site is paramagnetic or not, is due to the classic chemical exchange modulation of the scalar interaction between the protons in the bulk solvent and the observed ^{17}O nucleus. Surprisingly, there is a large change in this proton exchange rate when the apoenzyme is reconstituted with zinc or other metals. Studies as a function of pH demonstrate that the protein influences the transverse relaxation rate indirectly via the proton coupled exchange mechanism, over the range of physiological interest. Consequences of these results for the interpretation or reinterpretation of ^{17}O NMR data obtained using ^{17}O will be discussed.

W-AM-A2 DISSOCIATION AND OXYGEN-LINKED CHANGE OF THE QUATERNARY STRUCTURE OF AN ARTHROPODAN AND MOLLUSCAN HEMOCYANIN. Marius Brouwer* , Celia Bonaventura and Joseph Bonaventura. Duke University Marine Laboratory, Beaufort, North Carolina 28516.

1.Sedimentation analysis:The dissociation of 60S Limulus polyphemus hemocyanin was investigated as a function of pH,calcium ion concentration and ionic strength.Under the conditions used only three molecular weight species were present: 60S molecules,(48-mers),35S molecules (24-mers) and 5S molecules (monomers).The 60S molecule was stabilized by calcium,protons and high ionic strength.In contrast,the 100S α-hemocyanin of Helix pomatia was destabilized at high ionic strength.In the absence of calcium the 60S Limulus hemocyanin dissociated directly into monomers at alkaline pH. No intermediate 35S molecule was observed.

2.Kinetics of dissociation:60S Limulus hemocyanin was dissociated into 5S monomers and 100S Helix hemocyanin into 20S subunits by mixing with EDTA at pH 8.9.The dissociation process was studied by stopped-flow lightscattering.Under the conditions prior to mixing the oxygen binding by both hemocyanins was cooperative and the Limulus binding data could be described by the MWC model for allosteric transitions.The dissociation of both Limulus and Helix oxy-hemocyanin was heterogeneous(2.4 $\rightarrow$ 1.5 sec^{-1}; 75 $\rightarrow$ 20 sec^{-1}).The deoxy-hemocyanins mixed with deoxy-EDTA dissociated more slowly (1 $\rightarrow$ .4 sec^{-1} ; 40 $\rightarrow$ 4 sec^{-1}). This observation constitutes direct evidence for an oxygen-linked release of quaternary constraint of both hemocyanins upon the binding of oxygen.The time course of dissociation observed after mixing the deoxy-hemocyanins with an oxy-EDTA solution was the same as the time course of dissociation of the oxy-hemocyanins.This implies for both the arthropod and molluscan hemocyanin studied that the oxygen-linked change in quaternary structure(T $\rightarrow$ R transition) was complete within the dead time of the stopped-flow apparatus (2.3 msec) and therefore has an estimated first-order rate constant with a minimum value of approximately 2000 sec^{-1}.

W-AM-A3 ARTHROPOD HEMOCYANINS: FORMATION OF HYBRID OLIGOMERS WITH SUBUNITS FROM DIVERSE SPECIES. Michael Brenowitz, Celia Bonaventura and Joseph Bonaventura. Duke University Marine Laboratory, Beaufort, North Carolina 28516.

The functional and structural heterogeneity of the subunits of many arthropod hemocyanins is well established. That different subunits play unique roles in the assembly of the whole molecule has been demonstrated for hemocyanin of the horseshoe crab, Limulus polyphemus. We have determined that a reassembled 60S molecule of Limulus hemocyanin has a pH dependence of oxygen binding like that of the native 60S molecule, although it has a slightly increased oxygen affinity. Preliminary subunit composition analysis shows that the 9 bands discernable in regular gel electrophoresis are all present in the reassociated molecule and in about the same proportions. These results, together with electron microscopy of these 60S molecules, provide strong evidence that the reassembly yields products that are structurally and functionally similar to the native molecules. The hemocyanins of three other arthropods, the scorpion Androctonus australis garzonii, and the spiders Dugesiella californica and Cupiennius salei all have well characterized subunit structures. These species have maximum aggregation states with sedimentation coefficients of 37S, 37S and 24S respectively. The high molecular weight aggregates differ in oxygen affinity, cooperativity, and pH dependence (Limulus has a negative Bohr effect; Androctonus a positive Bohr effect). Hybrid interspecific oligomers can be assembled by substitution of hemocyanin subunits which are assembly homologues. The results add to our understanding of the structural and functional roles played by specific types of subunits. In particular, the maximum aggregation state attained by a given mixture is determined by the presence of specific subunit types.

W-AM-A4 MILLISECOND POLYMERIZATION STUDIES OF HEMOGLOBIN S. F.A. Ferrone, J. Hofrichter*, and W.A. Eaton, Laboratory of Chemical Physics, National Institutes of Health, Bethesda, Maryland, 20014.

By using laser photolysis of the carbon monoxide derivative of sickle-cell hemoglobin (HbS) we are able to induce polymerization of HbS in the millisecond regime. The polymerization is conveniently monitored by observing scattered photolysis light. The kinetic progress curves show a characteristic delay period as is seen by other techniques (which are presently confined to delay times greater than several seconds). By changing HbS concentration we are able to slow the polymerization to delay times of kiloseconds. The concentration dependence of the delay period remains high (40 to 50th power in HbS), similar to polymerization induced by temperature jump techniques. However, the shape of the progress curves is altered at short times, exhibiting a less abrupt onset of polymer formation. This short time behavior is closer to theoretical predictions for nucleated polymerization, and leads us to suggest that an additional process is operative at longer times by which the autocatalysis of polymerization is increased.

W-AM-A5 INTERACTION OF CALF BRAIN TUBULIN WITH POLYETHYLENE GLYCOLS. James C. Lee and Lucy L.Y. Lee*. Department of Biochemistry, St. Louis University School of Medicine, St. Louis, MO 63104.

Polyethylene glycols (PEG) have been shown to induce growth of crystals from a large variety of proteins and enhance tubulin self-assembly to microtubules. In order to elucidate the mechanism of this effect the partial specific volumes of calf brain tubulin were measured as a function of PEG molecular weight and concentration. Values of the apparent partial specific volume at constant chemical potential increased from 0.736 ml/gm to 0.782 ml/gm with increasing PEG concentration from 0 to 10% (w/v). With the application of multicomponent theory and assuming the value of the partial specific volume at constant chemical composition invariable, it showed that tubulin is preferentially hydrated, the magnitude of the effect increasing with PEG concentration and molecular weight. The chemical potentials of both the protein and PEG were raised indicating a destabilization of the system. Parallel measurements of the reactivity of sulfhydryl groups and apparent pK of tyrosine were designed to probe the structural integrity of tubulin. All sulfhydryl groups are available for chemical modification. The apparent pK of all tyrosine groups shifts from 10.9 to 11.2 upon transfering from buffer to PEG solutions indicating that the groups are less accessible to protons. (Supported by grants from Research Corporation and the American Heart Association, Missouri Affiliate, Inc.)

W-AM-A6 BRAIN CLATHRIN: BIOPHYSICAL AND ULTRASTRUCTURAL PROPERTIES
W. Bloom,* W. Schook,* C. Ores,* E. Feageson* and S. Puszkin, Department of Pathology, Mount Sinai School of Medicine of The City University of New York, New York, NY 10029

Brain clathrin is the protein believed to form baskets or cages around vesicles in brain. Brain nerve endings possess a large number of vesicles, many of them with surrounding basket structures. Clathrin was purified to homogeneity from enriched preparations of bovine brain coated vesicles fractions. The protein was separated from remaining vesicle membrane fragments using 2 M urea and Sepharose 4-B chromatography at pH 7.5. When the solution of clathrin was reduced in its pH from 7.5 to 6.5, numerous baskets or empty cages were formed (P.N. A.S., Jan. 1979, in press). Upon raising the pH back to 7.5, the baskets gave rise to filamentous structures. Filaments were cross-linked. The Stokes radius of clathrin was determined to be 140 Å. At pH 7.5, clathrin exhibited high intrinsic viscosity and low turbidity. At pH 6.5, viscosity dropped and turbidity increased. This increased turbidity was due to a decrease of filament cross-linking and basket formation as determined by electron microscopy. Upon raising the pH from 6.5 to 7.5, turbidity dropped and viscosity increased. Electron microscopy revealed that the linear structures of clathrin formed were followed by the disappearance of baskets. The raising and lowering of pH showed that filamentous structures originate from baskets and that baskets are formed from the cross-linked attachment of filaments. The changes observed were found to be reversible. The data suggest that clathrin participates with varied cytoskeletal structures in nerve-ending functions. The reversible structures are responding mainly to small pH changes in a manner similar to the way in which non-muscle actin structures are influenced by K^+ concentration and the microtubular system influenced by Ca^{2+}. S. Puszkin is Established Investigator of the American Heart Association and supported by grants #HL 20718, #NS 12467, #AA 03671 and the A.H.A.

W-AM-A7 A TWO CHAIN DNA HELIX WITH PHOSPHATES AT THE CENTER IS IN THE CORE OF PF1 VIRUS. L.A. Day, R.L. Wiseman & C.J. Marzec*. The Public Health Research Institute, New York, N.Y. 10016

Pf1 virus is 2.0×10^4 Å long and 60 Å in diameter. Its circular single-stranded DNA is arranged in the virion as two antiparallel chains in a cylindrical core of about 10 Å radius (D.A. Marvin & coworkers). There are 7400 nucleotides in the DNA and the protein coat consists primarily of about 7400 chemically identical subunits of 4609 daltons. The subunits presumably neutralize the phosphate charges. One nucleotide per protein subunit suggests that the DNA structure is closely related to the arrangement of subunits. If the subunits form a helix of 15 Å pitch with 5.4 subunits per turn, as indicated by the X-ray results of Marvin et al. and of L. Makowski & D.L.D. Caspar as well as physico-chemical results, then the two DNA chains would be in a helix of 15 Å pitch with 2.7 nucleotides per turn of each chain. Neighboring nucleotides in one chain would be related by a translation of $\sim$ 5.4 Å ($=2.0 \times 10^4$ Å/3700) and a rotation of 133° (=360°/2.7). From these parameters and a maximum phosphate-phosphate distance of 7.1 Å, one calculates that the phosphates are located at an average radius of 2.5 Å. It is conceivable, however, that the physical structure repeat is twice the crystallographic repeat due to the presence of a psuedo-dyad that is parallel to the structure axis. Were this true, the subunits could be on two parallel helices of 30 Å pitch and the antiparallel DNA chains could also have 30 Å pitch. In this case, the phosphates would be located at average radii ranging from 2.2 Å to 4.2 Å for phosphate-phosphate distances ranging from 5.9 Å to 7.1 Å. Thus, calculations for both 15 Å and 30 Å pitch models place the phosphates at the center. The results are consistent with spectral results which indicate that the bases are directed out and the phosphates in, and with published radial electron density distributions.

W-AM-A8 IN VITRO ASSEMBLY OF P22 PROHEADS FROM PURIFIED COAT AND SCAFFOLDING PROTEIN. M. Fuller, and J. King, M.I.T., Cambridge, MA 02139.

The double stranded DNA phages and some double stranded DNA animal viruses share a general mechanism of capsid morphogenisis. During the assembly of these viruses, an empty protein shell is formed, into which the DNA is later packaged. As yet, we know little about the mechanisms of initiation, subunit addition, vertex location and closure involved in the assembly of these icosahedral protein shells. We are studying the assembly of the prohead of bacteriophage P22. The prohead is a double shelled structure made of two major protein species, the coat protein, gp5 and the scaffolding protein, gp8. The scaffolding protein is required for the accurate assembly of the coat protein in vivo. During the DNA packaging the scaffolding protein exits from the virus structure and can participate in the assembly of additional proheads. We have developed procedures for the isolation of soluable coat and scaffolding protein from P22 proheads by selective dissociation of the shells with guanidine hydrochloride, followed by gel filtration and ion exchange chromatography. Both proteins obtained in this manner sedimented as monomers during sucrose gradient centrifugation. When the purified coat and scaffolding proteins were mixed at room temperature, they reassembled into structures with the same S value, protein ratio, and EM morphology as P22 proheads. When incubated separately under the same conditions, neither protein formed high molecular weight structures. Thus the prescence of the scaffolding protein is necessary for the assembly of the coat protein in vitro. The assembly reaction does not proceed at 4°c. Under these conditions both the coat and scaffolding protein remain monomers by sucrose gradient analysis. Using an in vitro DNA packaging system developed by Poteete, Jarvik and Botstein, we have been able to demonstrate the formation of complete, infective virus from the purified coat protein.

A-AM-A9 THEORY OF ELECTRICAL WORK AND SALTING-OUT IN TMV PROTEIN POLYMERIZATION. Max A. Lauffer, University of Pittsburgh, Pittsburgh, PA 15260.

The polymerization of TMV protein can be represented by $nA + mH^+ \rightarrow P$. Since charged particles are involved, $-RT\ln K_a' = \Delta G^o_{net}$ should be $\Delta G^o + \Delta W_{el}$, where ΔW_{el} is the difference between the electrical work of charging P and that of charging n A's.

$$\ln K_a' = \Delta S^o/R - (\Delta H^o + \Delta W_{el})/RT \quad (1)$$

When the apparent equilibrium constant is substituted for the equilibrium constant, K_a', a term in pH must be added, and when the equilibrium constant is converted to the concentration basis, K_c, an activity coefficient, γ, must be incorporated. When $\log\gamma = K_s'\mu$, the salting-out constant times ionic strength, (1) becomes

$$\ln K_c = \Delta S^o/R + 2.3nK_s'\mu - 2.3mpH - (\Delta H^o + \Delta W_{el})/RT. \quad (2)$$

Define T^* as the value of T when K_c has the value, K_c^*, and solve for $1/T^*$.

$$1/T^* = [\Delta S^o/n - (R/n)\ln K_c^* - 2.3R(m/n)pH + 2.3RK_s'\mu]/[\Delta H^o/n + \Delta W_{el}/n] \equiv \Delta S^*/[\Delta H^* + \Delta W_{el}^*] \quad (3)$$

When $\Delta W_{el}^*/\Delta H^*$ is much less than 1, when $\Delta S^{*\prime}$ is defined as $\Delta S^* - 2.3RK_s'\mu$ and when ΔW_{el}^* is a constant, ϕ, times charge per monomer, q, squared divided by $\sqrt{\mu}$,

$$1/T^* = \Delta S^{*\prime}/\Delta H^* + 4.57K_s'\mu/\Delta H^* - (\Delta S^{*\prime}/(\Delta H^*)^2)\phi q^2/\sqrt{\mu} \quad (4)$$

This simplifies to

$$1/T^* = C + B\mu - A/\sqrt{\mu} \quad (5)$$

When $\Delta S^{*\prime\prime}$ is defined as $\Delta S^* + 4.57(m/n)pH$, (3) becomes

$$(1/T^*)(1 + \Delta W_{el}^*/\Delta H^*) = (\Delta S^{*\prime\prime}/\Delta H^*) - 4.57(m/n)pH/\Delta H^*. \quad (6)$$

(5) can be used to interpret the effect of μ in terms of salting-out and electrical work. (6) can be used to evaluate ΔH^*, the enthalpy per mole of A, when m/n is known.

W-AM-A10 ELECTRICAL WORK IN EARLY STAGE POLYMERIZATION OF TMV PROTEIN. Ragaa A. Shalaby and Max A. Lauffer, University of Pittsburgh, Pittsburgh, PA 15260.

The entropy-driven polymerization of TMV protein is favored by an increase in ionic strength, μ, and by a decrease in pH. In addition to the salting-out effect, there is an effect attributable to electrical work, a function of both μ and pH. Ease of polymerization is measured in terms of a characteristic temperature, T^*, corresponding to the early stage in polymerization where the optical density increment from light scattering is 0.01. Theory shows that $1/T^*$ should vary with μ according to $C + B\mu - A/\sqrt{\mu}$ where C is the ratio of entropy to enthalpy, B is proportional to the salting-out constant divided by the enthalpy and $A/\sqrt{\mu}$ depends on the square of the charge and is proportional to the electrical work contribution divided by the enthalpy. Data in which μ varied from 0.025 to 0.15 obtained at pH 5.95, 6.35 and 6.50 were fitted successfully to this equation. Data were also obtained at a constant μ of 0.10 at pH values in increments of 0.1 from 5.9 to 6.8. Theory predicts that $1/T^*$, corrected for the electrical work contribution, should be a linear function of pH with a negative slope proportional to the ratio of the number of hydrogen ions bound per protein unit during polymerization to the enthalpy. The data permit evaluation of the enthalpy to be 29.7 kcal/mole. With this value, the parameters C,B and A can be interpreted. Standard entropies range from 106 at pH 5.95 to 103 e.u. at pH 6.50. The salting-out constant is 2.6 at all pH values. The electrical work contribution at μ = 0.10 is 0.357, 0.545 and 0.640 kcal/mole at pH 5.95, 6.35, 6.50, respectively. Theoretical calculations from models yield values in agreement within a factor of two.

W-AM-A11 SPEED DEPENDENCE AND WALL EFFECTS FOR SEDIMENTATION OF MAMMALIAN CELL DUPLEX DNA IN NEUTRAL SUCROSE GRADIENTS. R. Chen* and A. Cole (Intr. by R. E. Meyn), University of Texas System Cancer Center, M. D. Anderson Hospital and Tumor Institute, Texas Medical Center, Houston, TX 77030.

Duplex DNA from gently lysed CHO cells was sedimented through sucrose gradients containing 5M NaCl. $S_{20,w}$ values corresponding to the peaks of the profiles and number average molecular weights were determined for spin speeds between 2.9 and 26 Krpm. Only small dependences on spin speed were observed below 10 Krpm although profound decreases occurred at higher speeds. Comparable profiles were obtained for sedimentation in 38 ml polyalomer tubes and in specially constructed 10 ml straight-wall and 6 ml sectored-wall teflon tubes; indicating that strongly perturbing wall effects were not present. The profile was not significantly changed when the spin period was split by an 18 hour rest period indicating that diffusion of DNA or sucrose during that period was negligible. These results support studies on the properties of mammalian cell duplex DNA which we have reported previously. Supported in part by Department of Energy Contract EY-76-S-05-2832.

W-AM-A12 MELTING PROFILES OF BASE PAIRS IN THE LACTOSE OPERON PROMOTER BELOW THE HELIX COIL TRANSITION TEMPERATURE. A. S. Benight* and R. M. Wartell, Georgia Institute of Technology, Atlanta, Georgia 30332.

We have calculated the melting profile at 40°C and 60°C for a 200 base pair sequence of the lactose operon surrounding the start point for transcription. Parameter values used were obtained empirically from DNA melting curves in 0.2 M Na^+. The modified Ising model, including the effect that the stacking interactions differ for different types and orientations of stacked base pairs, has been employed. Estimates of ten different stacking interactions were obtained by analysis of Tm values for synthetic DNA polymers and several sets of assumptions. Realistic changes in these assumptions did not significantly alter the melting profile. Calculations show that the major influence of a base pair's stability depends on the base pair type. The average probability of melting an A·T at 40°C and 60°C is approximately 3.6×10^{-4} and 9.6×10^{-4} respectively. For a G·C base pair the average probability of melting at 40°C and 60°C is 6.7×10^{-5} and 1.9×10^{-4} respectively. However, different sequence environment alters the probability of melting by about 25%. The UV5, p^S, p^r1a, L8 and L157 promoter mutations at 40°C and 60°C decreased the stability of the region of their occurrence. At 40°C all mutations decreased the stability by about 1.1 kcal. At 60°C the decrease in stability varied from 1.2 kcal to 1.6 kcal depending on the mutation.

W-AM-A13 INTERACTION BETWEEN POLYTRIPEPTIDE COLLAGEN MODELS AND GLYCOSAMINOGLYCANS. C.M. Balik and A.J. Hopfinger, Department of Macromolecular Science, Case Western Reserve University, Cleveland, OH. 44106

Glycosaminoglycans, such as chondroitin-6 and chondroitin-4 sulfate, are components of the "ground substance" of connective tissue, and interact with collagen fibers to form a strong fiber-matrix composite. The molecular features of this interaction are not known. We have attempted to model this interaction by using chondroitin sulfates and polytripeptides, such as $(Gly\text{-}L\text{-}Pro\text{-}L\text{-}Pro)_x$, which can form triple helices in solution which are believed to be structurally similar to collagen. Use of these polytripeptides in lieu of collagen simplifies the problem, since their primary structure is well-defined and constant, whereas that of collagen is not. Experimentally, films were cast from dilute solution containing both the polysaccharide and the polytripeptide and analysed using Fourier-transform infrared spectroscopy (FTIR). FTIR difference spectra obtained by subtracting a non-interacting mixture spectrum from an interacting (co-cast) spectrum of the same composition suggest that some interaction does indeed occur. Possible models for this interaction, consistent with theoretical intermolecular structure calculations, will be discussed.

W-AM-A14 A MODEL FOR SUPERFOLDING OF DNA IN CHROMATIN. N. Yathindra* (Intr. M. Sundaralingam), Department of Biophysics, University of Madras, Madras, India.

A model for super helical DNA in chromatin is proposed by postulating that chromatin DNA may be regarded as a polymer chain comprising "10 base-paired B-DNA" as the repeating monomer unit and that the tertiary folding of DNA may be achieved by small conformational changes in the ester P-O bonds which link the successive "10 base-paired" secondary structural units. The distinct dissimilarity, though small, between the P-O torsions at the junctions of the repeating B-DNA units and those within them is sufficient to produce smooth bends which facilitates DNA to superfold into a compact structure. This model, while preserving the symmetry of the B-DNA structure, introduces "kinks" at intervals of 10n phosphodiesters (base pairs) and does not call for any abrupt conformational changes or unstacking of the bases. This model naturally accounts for the 10 base-paired repeat implied by the nuclease digestion studies. Super helical parameters (n, the number of repeating B-DNA units per turn and h, the height per residue along the super helical axis) are computed by using a scheme of "extended single virtual bonds" to investigate the possible super helical structures. 70 to 100 base-pairs can be accommodated per super helical turn with a pitch of 28Å and radii varying from 30-50Å. Super helices having more than 100 base-pairs/turn are found to have radii greater than 70Å and are not compatible with the known nucleosome dimensions. Both left-handed and right-handed super helical structures can be obtained by relatively minor changes in rotations about the P-O bonds linking the "10 base-paired B-DNA" secondary structural segments. An interesting stereochemical outcome of this study is that the conformational structures of even super helical nucleic acids can be stereochemically characterized using the rigid nucleotide concept.

W-AM-B1 INTERACTION OF SMALL MOLECULES WITH LIPOSOMES:PERMEABILITY STUDIES. M.A. Singer, Dept. of Medicine, Queen's University, Kingston, Ontario, Canada K7L 3N6

In a previous study the effects of a series of benzene and adamantane derivatives on fatty acyl chain motion were examined in spin labelled liposomes composed of saturated Phospholipids. All of these compounds increased lipid chain motion below the phospholipid Tc, but the magnitude of this increase depended upon the presence or absence of polar groups, their type and position. In the present study an attempt was made to correlate these observations with the effects of these same compounds on glucose and sodium effluxes from similar liposomes. Multilamellar liposomes were formed from either dimyristoyl phosphatidylcholine (PC) or dipalmitoyl PC plus a small amount of dicetylphosphate (DCP) and loaded with either ^{22}Na or (^{14}C) glucose. The leak of these isotopes was used as a measure of permeability. In some experiments unlabelled glucose was used and measured enzymatically. Both lipids display a permeability maximum in the region of the Tc. However dimyristoyl PC liposomes become much more permeable than those composed of dipalmitoyl PC. Furthermore in dimyristoyl PC vesicles glucose and sodium effluxes are approximately equivalent whereas glucose efflux is greater than sodium efflux in dipalmitoyl PC liposomes. Overall there was a poor correlation between the effects of these compounds on fatty acyl chain motion and on permeability. Many compounds did increase the efflux rate below the Tc in dimyristoyl PC vesicles but did not have a similar effect on dipalmitoyl PC vesicles. Two additives in particular, butylated hydroxytoluene (BHT) and p-di-t-butylbenzene (DBB) actually decreased permeability in both lipids. BHT probably alters the interfacial region, but not its dipole potential since it decreased both glucose and sodium effluxes, while DBB probably increases bilayer thickness. (Supported by MRC)

W-AM-B2 EFFECT OF PHLORETIN ANALOGUES ON ION TRANSPORT. R. Latorre, J. Reyes*, R. Motais* and D. C. Tosteson, Dept. of Physiology, Harvard Medical School, Boston, Mass. 02115 and Faculte des Sciences, Universite de Nice, France.

In order to further clarify the physicochemical mechanisms responsible for the phloretin effects on cell transport processes, we have studied the effects on ion transport of various phloretin analogues with different dipole moments and different hydrophobicities in planar lipid bilayer membranes. In this study, we measured the changes in the transport characteristics of a lipophilic cation (tetraphenylarsonium) and of a lipophilic anion (tetraphenylborate) induced by the addition of phloretin analogues to the aqueous phases bathing a phosphatidylethanolamine bilayer. The strategy has been as follows: we considered phloretin as a derivative of the acetophenone containing two kinds of substituents--one on the ring and another on the carbon chain. By introducing different kinds of substituents in either the ring or the carbon chain, phloretin analogues with the same dipole moment as phloretin but different hydrophobicities, or phloretin analogues with different dipole moments and hydrophobicities are obtained. For all the phloretin analogues tested, we found: 1)an increase in cation permeability and a decrease in anion permeability; 2)the change in membrane dipole potential as inferred from the changes in ion permeabilities are proportional to the dipole moment of the phloretin analogue and to its absorption coefficient in the membrane; and 3)once corrected by their adsorption coefficient, molecules with the same dipole moment are able to promote similar changes of the membrane dipole potential. The decrease in membrane dipole potential promoted by these compounds as measured in lipid bilayers correlates well with the ability of phloretin analogues in inhibiting the chloride transport in red blood cells. Supported by NIH Grant GM-25277.

W-AM-B3 TEMPERATURE-JUMP STUDY OF THE BINDING KINETICS OF PHLORETIN TO PHOSPHATIDYLCHOLINE (PC) VESICLES. A. S. Verkman and A. K. Solomon, Biophysical Laboratory, Harvard Medical School, Boston, MA 02115.

The sub-millisecond kinetics for phloretin binding to unilamellar PC vesicles was investigated using the temperature-jump technique. Spectrophotometric studies of the equilibrium binding were also performed at 328 nm and demonstrated that phloretin binds to a single set of independent equivalent sites on the vesicle with a dissociation constant of 8.0 μM and a lipid/site ratio of 3.8. The temperature of the phloretin-vesicle solution was jumped by 4°C within 3 μsec which revealed a mono-exponential, concentration-dependent relaxation process with time constants in the 30-200 μsec time range. An analysis of the concentration dependence of relaxation time constants yielded a 3.9×10^8/M-sec binding rate constant and a 3500/sec debinding constant; ca. 45% of total binding sites are exposed at the outer vesicle surface. The binding rate constant is consistent with diffusion limited kinetics. This is further substantiated by 2 additional observations. The phloretin analogue, naringinin, (dissociation constant, 24 μM) bound to PC vesicles with the same rate constant as phloretin did. Hence, the binding rate constant is dependent upon the diffusion coefficient in the buffer and is not altered by differences in binding affinity. In addition, the phloretin-PC system was studied in buffers made 1-6 times more viscous than water by addition of sucrose or glycerol. The equilibrium affinity for phloretin binding to PC vesicles is independent of viscosity, yet the binding rate constant decreases with the expected dependence ($k_{binding} \propto 1/viscosity$) for diffusion limited processes.

(Supported in part by NIH grant GM 15692).

W-AM-B4 NET PROTON-HYDROXYL PERMEABILITY OF LIPOSOMES. J.W. Nichols and D.W. Deamer, University of California, Davis, Calif. 95616

The net permeability of protons and hydroxyls (P_{net}) has been measured in ether injected liposomes.(Deamer and Bangham, BBA, 443 (1976)) Liposomes were prepared so that they contained a highly buffered(150 mM ACES) solution internally and a lightly buffered isosmotic (1.5 mM ACES) solution externally. These liposomes were placed in a small vial and continuosly flushed with argon to remove CO_2 while the external pH was monitored by a glass pH electrode. A small acid or base pulse establishes a pH gradient (0.1-0.2 pH units) across the membrane. From the initial rate of return to equilibrium ($\Delta pH/\Delta t$), the net flux of protons and hydroxyls can be calculated. Addition of valinomycin served to short circuit any electrical potential so that the flux could be expressed as a function of the activity differences of protons and hydroxyls: $J_{net} = P_H(\Delta[H^+]) + P_{OH}(\Delta[OH^-])$. For a small pH pulse around 7.0, $\Delta[H^+] = \Delta[OH^-]$ such that $J_{net} = (P_H + P_{OH})(\Delta[H^+])$ or $J_{net} = P_{net}(\Delta[H^+])$. For five independent trials, we calculated $P_{net} = 2.2 \times 10^{-4} \pm 1.5 \times 10^{-4}$ cm/sec. P_{net} measured by a completely independent method using a large pH gradient ($\Delta pH=3$) and 9-aminoacridine to measure the net proton-hydroxyl flux rate is one order of magnitude smaller. (Nichols and Deamer, Proc. of the Frontiers of Biological Energetics, 1978). Both values are 10^6 to 10^7 times greater than the permeability of Na^+ and K^+ in comparable liposomes. This high permeability may be a result of proton and hydroxyl interaction with clusters of water molecules in the hydrocarbon region of the lipid bilayer. We have investigated the solubility of water in cis-5 decene and found it to be 200 times that of trans-5 decene or decane. The increased solubility of water in cis double bonded alkyl chains should be reflected in egg lecithin liposomes and may account for the high net proton-hydroxyl permeability.

W-AM-B5 CONFORMATION OF GRAMICIDIN A CHANNEL IN LIPID VESICLES: A ^{13}C and ^{19}F NUCLEAR MAGNETIC RESONANCE STUDY. W. Veatch, S. Weinstein*, B.A. Wallace, J. Morrow†, and E.R. Blout*, Harvard Medical School, Boston, Mass. 02115 and †Yale Medical School, New Haven, Conn. 06520.

We have determined the conformation of the channel forming polypeptide antibiotic gramicidin A in phosphatidyl choline vesicles using ^{13}C and ^{19}F nuclear magnetic resonance. Independent evidence suggests that gramicidin A in these lipid vesicles is in the form of dimer transmembrane channels. Models previously proposed for the conformation of the dimer channel differ in the surface localization of the N- and C-termini. The N-terminal to N-terminal helical dimer has only the C-termini on the surface of the membrane, while the C-terminal to C-terminal helical dimer has only the N-termini at the surface. All parallel and antiparallel-β double helices have both the N- and C-termini on the surface. We have incorporated specific ^{13}C and ^{19}F nuclei at both the N- and C-terminus of gramicidin and have used ^{13}C and ^{19}F chemical shifts and spin lattice relaxation time measurements to determine the accessibility of these labels to three paramagnetic nmr probes. Two of the probes are in the solution--thullium ion (Tm^{+++}) and manganese ion (Mn^{++}), neither of which is transported by the channel,--and one is a nitroxide spin label attached specifically near the end of a phosphatidyl choline fatty acid chain. Formyl Val_1 was removed from the N-terminus of the peptide and replaced by ^{13}C-enriched Formyl-Val_1. The C-terminus was labelled by O-acetylation (^{13}C methyl). All of the results imply that the C-terminus of gramicidin in the channel is at the surface and the N-terminus is buried near the center of the membrane. These data strongly favor the N-terminal to N-terminal helical dimer and exclude the C-terminal to C-terminal dimer and all of the double helices as major conformations for the gramicidin channel in phosphatidyl choline vesicles.

W-AM-B6 NUCLEAR MAGNETIC RESONANCE STUDIES OF THE PERMEATION OF SMALL SOLUTES THROUGH LARGE UNILAMELLAR VESICLES. J. R. Alger* and J. H. Prestegard, Yale University, New Haven, Ct., 06520.

Magnetization transfer nuclear magnetic resonance (nmr) and analysis of nmr line shapes are applied to the measurement of the rates at which small molecules permeate membranes. The methods are advantageous in that time scales of 0.001 to 1.0 seconds are accessible, and that a net gradient in concentration across the membrane is not required. The permeation of acetic acid through large unilamellar phospholipid vesicular membranes serves as a model system for illustration of the procedures. The permeation rate dependence on pH, total acid concentration and membrane head group structure is reported. These data allow proposal of a detailed molecular mechanism for the acetic acid permeation process.

W-AM-B7 CO-TRANSPORT OF CATIONS AND ANIONS ACROSS LIPID BILAYERS MEDIATED BY A NEUTRAL CARRIER--A MODEL FOR BIOLOGICAL SYMPORT SYSTEMS. R. Margalit and G. Eisenman, Physiol. Dept., UCLA Medical School, Los Angeles, Ca. 90024.

Moyle and Mitchell (Febs Lett. 84:135, 1977) have suggested the existence of calcium-anion symporters Ca_2^{4+}-HPO_4^{2-} and Ca^{2+}-β hydroxybutyrate$^-$. We found Simon's Li^+-selective complexone to form complexes with cations or anions in bilayers (Margalit and Eisenman, Arzneim.-Forsch./ Drug Res. 28, 705 (1978)); and we here report that it can also act as a symporter of charged cation-anion complexes. Pure cation (I^+), anion (A^-), and carrier (S) complexes having stoichiometries IS^+, IS_2^+, AS^-, $A_2S_2^{2-}$ are unambiguously identified for aqueous carrier conc. of 10^{-8}-10^{-6}M from 1st and 2nd power dependences of conductance on conc. together with dilution potential behavior characteristic of a single permeant species. However, for higher carrier conc. (10^{-6}-10^{-4}M), 3rd and 4th power dependences of membrane conductance on salt and carrier conc. are observed; and the dilution potentials correspond to those for a mixture of permeant species of varying stoichiometries. Although it is difficult from electrical data alone to establish uniquely the stoichiometry of each complex in a mixture, the data in LiCl suggest the coexistence of the pure cation complex LiS_2^+ and the symport complex $Li_2ClS_4^+$. The data in $CaCl_2$ indicate the coexistence of the pure anion complex $Cl_2S_2^{2-}$ and the symport complex $Ca_2Cl_2S_4^{2+}$. Pleasingly, the symport complexes consist of aggregates of the complexes pre-existing at lower carrier conc. stabilized by counterions. For example, the postulated symport complex $Li_2ClS_4^+$ consists of two LiS_2^+ complexes held together by a Cl^-; whereas the symport complex $Ca_2Cl_2S_4^{2+}$ consists of a $Cl_2S_2^{2-}$ complex whose anions are screened by Ca^{++} and S (see Diagrams).

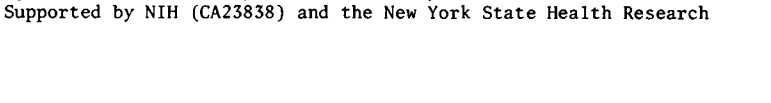

Supp. by NSF (PCM762-0605), USPHS (GM24749).

W-AM-B8 FLUORESCENCE AND LIGHT SCATTERING STUDY OF THE INTERACTION OF PHOSPHOLIPID BILAYERS. G. A. Gibson, L. M. Loew, Department of Chemistry, S.U.N.Y. at Binghamton, Binghamton, New York 13901.

The derivatized phospholipids dansyl-dipalmitoyl-phosphatidylethanolamine (DDPPE) and rhodamine-B-dipalmitoyl-phosphatidylethanolamine thiourea (Rh-B-DPPE) have been used to investigate time dependent processes occurring in several phospholipid dispersions. These two probe molecules interact by the Forster resonance energy transfer mechanism with Rh-B-DPPE quenching the fluorescence of DDPPE. A He-Cd laser (325 nm) is used for excitation of the latter probe and scattering from vesicles. Fluorescence intensity at the fluorescent maxima for each probe or the ratio of these intensities can thus be observed simultaniously with the Rayleigh scattering. Rayleigh scattering has been used extensively to measure the rate of fusion of phospholipid vesicles. The fluorescence quenching method that we emply is sensitive not only to fusion but also to aggregation events. This is due to the long range nature (theoretically, R_o=65Å for our probes) of the Forster process. Differences, then, between the kinetic behavior as observed by Rayleigh scattering and that observed by fluorescence may be attributed to a non-fusion interaction event. Supported by NIH (CA23838) and the New York State Health Research Council (#362).

W-AM-B9 EVIDENCE FOR POSSIBLE ROLE OF PHOSPHATIDYLETHANOLAMINE AS A MODULATOR OF MEMBRANE-MEMBRANE CONTACT. Michael A. Kolber* and Duncan H. Haynes, Dept. Pharm., Univ. of Miami, Miami, Fl.

Phosphatidyl ethanolamine (PE) and PE/PC (phosphatidyl choline) stable vesicle populations can be prepared at pH 9.5. When the pH is reduced to 7.0 the vesicles aggregate. The kinetics and equilibria of aggregation were studied in stopped-flow rapid mixing experiments. The aggregation process has a highly sigmoidal dependence on H^+ concentration with the critical pH for aggregation lying near 7.0. This is explained by the requirement of protonation of a minimal interaction area for aggregation to occur. In the fully protonated state a high equilibrium constant for aggregation (K_{eq}) is obtained, indicating possible intervesicular head-to-tail binding and possible hydrogen bonding between lipid polar heads. Vesicles containing PC habe a decreased tendency to aggregate.

Although the high K_{eq} of PE vesicles may provide the forces that maintain stable aggregation of membranes stopped-flow studies show that the rate constant for aggregation is two orders of magnitude below that for diffusion controlled aggregation. These observations suggest that although PE is capable of stabilizing membrane-membrane contact, it is not capable of rapid ($t_{1/2}$ < 1 msec) initiation of contact. It would appear that PE can play a modulatory role.

An equilibrium model is presented describing the PE induced aggregation phenomenon in terms of three parameters: the equilibrium constant for the protonation of the PE (K_A), K_{eq} and the number of PE molecules in an effective interaction area that the two vesicles must interact in order to aggregate (N_{eff}).

This work was supported by NIH Grants HL 16117, AI 20086, GM 23990, H 123392 and NIH Training Grant No. HL 07188-3.

W-AM-B10 1. EFFECT OF TEMPERATURE ON VESICLE AGGREGATION

J. Bentz* and S. Nir (Intr. by M. Andersen) Roswell Park Memorial Institute, Buffalo, N.Y. 14263 and Dept. of Biophysical Sciences, SUNYAB

Detailed binding studies (1) enabled us to calculate the concentrations of Na^+ required to yield measurable aggregation of sonicated phosphatidylserine (PS) vesicles. The rates of aggregation of these vesicles are calculated according to the Smoluchowski-Fuchs theory from potential curves obtained as a sum of Van der Waals and electrostatic interactions. The effect of temperature on the rates of aggregation and on the equilibrium distribution is analyzed. Light scattering results (2) confirm the expectation that the equilibrium distribution of these vesicles would favor a higher degree of aggregation at low temperatures. The calculations indicate that the rate of the dimerization reaction should increase with temperature. However, it has been observed that the rate of increase of light scattered by aggregating PS vesicles decreases as the temperature is raised from 10^o to 30^o. Thus, it was concluded that the half time of aggregation, obtained as the time of a 50% increase of scattered light over the initial dispersed state, requires consideration of both the backward reaction (dimer→monomer + monomer) and higher order aggregates. The analysis has been extended in this direction.

Supported by NIH grant GM23859-1

References

1) Nir, S., C. Newton, and D. Papahadjopoulous, Bioelectrochemistry and Bioenergetics, 5, 116,(1978); Kurland, R., C. Newton, S. Nir, and D. Papahadjopoulous, Biochim. Biophys. Acta, in press

2) Nir S., J. Bentz, and A. Portis, Submitted to Advan. in Chemistry

W-AM-B11 1. PROMOTION AND INHIBITION OF AGGREGATION AND FUSION OF ACIDIC PHOSPHOLIPID VESICLES BY CATIONS

S. Nir, J. Bentz and A.R. Portis, Jr., Roswell Park Memorial Insittute, Buffalo, N.Y.14263

Rates of aggregation of acidic phospholipid vesicles are calculated from potential curves obtained as a sum of Van der Waals and electrostatic interactions. The effects of cation binding (Ca^{2+}, Mg^{2+} and Na^+) to phosphatidylserine (PS) vesicles are analyzed, and the rates of vesicle aggregation are shown to be very sensitive to cation concentration. Calculations are related to data obtained from light scattering and release of trapped fluorescent molecules. In those cases for which membrane fusion has been previously demonstrated, the results show an increase in light scattering and a fast release of fluorescent molecules-indicative of aggregation and fusion. High concentrations of Na^+ inhibit the fusion process, although Na^+ alone (>.4M) induces fast aggregation. The calculations, as well as previous binding studies (1), show the dependence of the amount of Ca^{2+} or Mg^{2+} bound to PS on the Na^+ concentration. The possibility is raised that Ca^{2+} or Mg^{2+} can produce destabilization of PS vesicles followed by aggregation and fusion, requiring some critical threshold ratios of divalent cation bound per PS. This hypothesis is also supported by the fact that significant vesicle aggregation and release of trapped fluorescent molecules are observed with Ca^{2+} or Mg^{2+} solutions under conditions of very low ionic strength, where the calculations indicate a very slow rate of close approach for intact vesicles. The conclusion is that in the presence of Ca^{2+} or Mg^{2+} and low Na^+ the amount of divalent cation bound exceeds the critical threshold; and that the vesicles are destabilized in some fashion which promotes their aggregation and fusion. Supported by NIH grants GM23850-01 and GM18527, CA 05467 and ICRETT and ICRDB, NO1-CO-65341.

1) S. Nir, C. Newton, D. Papahadjopoulos, Bioelectrochemistry and Bioenergetics, 5,116(1978)

W-AM-B12 1. EFFECT OF CATIONS ON PHASE TRANSITIONS OF PHOSPHATIDYLSERINE: COMPETITION AND SYNERGISM.

M.M. Hammoudah, S. Nir, J. Bentz (Intr. by R. Kurland), Roswell Park Memorial Institute, Buffalo, NY 14263.

Phase transition changes as a result of interactions of cations with multilamellar phosphatidyl serine (PS) vesicles have been studied employing differential scanning calorimetry (DSC) and binding calculations. An increase in Na^+ concentration from .1 to 1M introduces a shift in the phase transition temperature Tm by about 5^oC. The rare earth cations La^{3+} and Gd^{3+} produce a transition shift of about 25-30^oC when added in concentrations of about 0.1 to 0.5mM. The phase changes induced by trivalent cations are only slightly affected by the addition of Na^+ up to 1M. Binding studies (1) of Ca^{2+} in the presence of Mg^{2+} indicate that Ca^{2+} is highly effective in competing and displacing Mg^{2+} from PS vesicles. The thermotropic phase transition of PS in the presence of .1M Na^+ and 0.15mM Ca^{2+} (initially present) is shifted to very high temperature, whereas in the presence of several mM/mg^{2+} the shift is by about 10-15^oC. Recently (2) it was repeated that for a certain range of concentrations more Ca^{2+} is bound to PS in the presence of Mg^{2+} than in its absence. In the present study, we found that in the presence of 1M Na^+ or .2mM La^{3+}+.1M Na^+ Tm increases by 5 and 25^oC, respectively; however, in these two cases the addition of .2mM Ca^{2+} did not produce an additional increase in Tm. Presumably, Na^+ or La^{3+} at the above concentrations compete effectively with Ca^{2+} for binding to PS. We are now examining whether the marked effect of Ca^{2+} on the phase transitions in these cases is a slow process which would only appear after long incubations with Ca^{2+}. Supported by NIH Grant GM23850-01 and by Institutional Research Grant IN-54 R-17 of ACS. References: (1) C.Newton, W.Pangborn, S.Nir, D. Papahadjopoulos, Biochem. Biophys. Acta 506, 281 (1978).(2) A.Portis, C.Newton, W. Pangborn, D.Papahadjopoulos, Biochemistry, in press.

W-AM-B13 THE ADSORPTION OF ALKALI METAL CATIONS TO BILAYER MEMBRANES CONTAINING PHOSPHATIDYL SERINE. Stuart McLaughlin and Moises Eisenberg*, HSC, SUNY Stony Brook, N.Y. 11794

We made (i) electrophoretic mobility measurements on multilamellar vesicles to determine the zeta potential, the electrostatic potential at the hydrodynamic plane of shear; (ii) fluorescence measurements with TNS on sonicated vesicles to determine the potential at the surface of the bilayer; (iii) conductance measurements with carriers on planar black lipid membranes to determine the potential in the center of the membrane. These measurements demonstrate that the association constants of monovalent cations with phosphatidyl serine decrease in the sequence Tris>Li>Na>NH_4>K>Rb>Cs>TEA>TMA. The Stern equation, a combination of the Langmuir adsorption isotherm, the Boltzmann relation and the Gouy equation from the theory of the diffuse double layer can describe, in a self consistent manner, all the data we have obtained. Electrophoretic mobility measurements on vesicles containing mixtures of the negative lipid phosphatidyl serine and the zwitterionic lipid phosphatidyl choline indicate that the plane of shear is within two Angstroms of the surface of the bilayer membrane and that the zeta potential is, therefore, an excellent approximation to the surface potential under all the experimental conditions we have examined (1<[Na],[TMA]<100 mM). Under most conditions the zeta potential can be calculated from the electrophoretic mobility by the classical Helmholtz-Smoluchowski equation, but when the potential is high (>100 mV) and the salt concentration is low (<10 mM) the relaxation of the ionic double layer becomes significant for small vesicles and the equations of Wiersema, Loeb and Overbeek (1966) must be used. When the adsorption of monovalent cations is taken into account, the binding of calcium and magnesium to membranes containing phosphatidyl serine can also be described by the Stern equation. Supported by NIH grant GM24971 and NSF grant PCM76-04363 to S. McL.

W-AM-B14 PARTICLE-ENHANCED TRANSPORT OF CHEMICAL CARCINOGENS STUDIED BY FLUORESCENCE SPECTROSCOPY. J.R. Lakowicz and D.R. Bevan,* University of Minnesota, Navarre, MN, 55392.

It is known from human epidemiological evidence and from experimental animal studies that particulate materials such as asbestos and hematite are highly co-carcinogenic with polynuclear aromatic hydrocarbons (PAH). Thus, we undertook studies to elucidate one possible molecular mechanism for this phenomenon, namely the particle-mediated uptake of PAH into model membranes, microsomes, and cells. Fluorescence spectroscopy was used to measure the surface distribution of the PAH on the particulates as well as the kinetics of transfer of the PAH from the particulates to the membranes. The fluorescence emission spectra and apparent quantum yields of the PAH are highly dependent on the physical form of the PAH and their immediate local environments. Thus, from the fluorescence emission it was possible to obtain information concerning the ability of the particulates to disperse the PAH in a monomeric state as opposed to the microcrystalline state. It was found that this ability is more dependent on the surface properties of the particulate than on its surface area. In addition, the kinetics of uptake of the PAH was measured by monitoring the increase in fluorescence intensity of the PAH upon transfer from the particulate-bound state to the nonpolar region of the membranes. It was determined that particulates in general, irrespective of chemical composition, enhance the rate of membrane uptake of PAH. In particular, it was found that the fibrous minerals such as the chrysotile and anthophyllite forms of asbestos show greater enhancement of the transport than do the non-fibrous minerals such as hematite and silica. These findings may provide a partial for the co-carcinogenic effects of PAH and particulates.

W-AM-B15 3′-PYRENEMETHYL-23,24-dinor-5-CHOLEN-20-ATE-3β-OL OLEATE: A FLUORESCENT PROBE FOR MONITORING FUSION OF UNILAMELLAR PHOSPHOLIPID VESICLES D.P. Via*, Y.J. Kao* and L.C. Smith, Baylor College of Medicine, Houston, Texas 77030

A new fluorescent cholesterol ester analog, 3′-pyrenemethyl-23,24-dinor-5-cholen-20-ate-3β-ol (PMCA oleate) exhibited characteristic pyrene photophysics in sonicated unilamellar phospholipid vesicles with monomer fluorescence emission at 390 nm and excimer fluorescence at 475 nm. The ratio of excimer to monomer fluorescence (E/M) was linear with increasing PMCA-oleate concentration in phosphatidylcholine (PC), phosphatidylserine (PS), and phosphatidylglycerol (PG) vesicles. No exchange of the steryl ester probe occurred between labeled vesicles and a 10-fold excess of unlabeled vesicles after 4 hr. at 37°C. Fusion of PS or PG vesicles containing 2 mole % PMCA-oleate with unlabeled acceptor vesicles was initiated by divalent cations. The decrease in the E/M ratio depended upon both the divalent cation concentration and the relative proportion of acceptor and donor vesicles. Fluorescence changes were maximal at 5 mM Ca^{++} or 12 mM Mg^{++} for PS and 30 mM Ca^{++} or 50 mM Mg^{++} for PG vesicles. Divalent cations had no effect on the E/M ratio of labeled PC vesicles. 1-Monoacyl PC and fatty acids did not cause fusion, judged by the absence of significant changes of the E/M ratio of PMCA-oleate in either PS, PG or PC vesicles. 1 Monoacyl PC (10 mole %) added to the preformed PS or PG vesicles prevented subsequent cation induced decline in E/M ratio. By stopped-flow spectrophotometry, the rates of cation mediated fluorescence and light scattering changes were dependent on the specific phospholipid and the specific cation, with half-times that ranged between < 2 msec to 10 sec. (Robert A. Welch Q-343, USPHS HL-07282, HL-15648, HL-17269).

W-AM-B16 EFFECTS OF DIVALENT IONS ON VESICLE-VESICLE FUSION STUDIED BY A NEW LUMINESCENCE ASSAY FOR FUSION. Ronald W. Holz and Carol A. Stratford. University of Michigan Medical School, Ann Arbor, Michigan 48104.

A new assay has been developed for vesicle-vesicle fusion based upon the mixing of intravesicular contents of two sets of vesicle. Purified firefly luciferase and $MgCl_2$ were incorporated into one set of vesicles (LV) and ATP into the other (AV). Vesicles were prepared from soybean phospholipids. The luminescence that resulted from hydrolysis of ATP by luciferase was measured to determine the extent of mixing of the intravesicular contents. In the absence of divalent ions, incubation of a mixture of LV and AV did not produce luminescence. However, if Ca^{++} or other divalent ions were present at millimolar concentrations, luminescence occurred. The luminescence did not result from extravesicular reaction of vesicle contents that had leaked into the medium. Instead, luminescence resulted from the mixing of intravesicular spaces of AV and LV in fused vesicles. Optical density changes and negative stain electron microscopy indicated that Ca^{++}-induced extensive aggregation of vesicles. However, quantitation of the maximum possible luminescence indicates that only a small percentage (less than 1%) of the vesicles actually fused in a fusion experiment. Addition of EDTA to chelate Ca^{++} after luminescence had been induced resulted in a 2-3 fold increase in light emission which then rapidly decayed. These results suggest that the sudden removal of Ca^{++} caused a transient increase in fusion after which subsequent fusion was inhibited. It was also found that the vesicles were relatively stable to hypotonic solutions.

W-AM-C1 PHYSIOLOGICAL RELEVANCE OF THE ATP DEPENDENT Ca PUMP IN SQUID AXONS. R. DiPolo and L.A. Beaugé, IVIC, Apartado 1827, Caracas 101, Venezuela. Dept. Biophysics, University of Maryland, Baltimore, U.S.A.

It has been shown (DiPolo, Nature 274:390, 1978), that in the absence of a Na gradient, squid axons can promote an ATP dependent net Ca extrusion which occurs independently of Na_o, Ca_o and Mg_o ('uncoupled pump'). In this work, we have explored the physiological relevance of this finding by studing the effect of ATP, Na_i, Na_o and Ca_o on Ca efflux at different $[Ca^{++}]_i$. Squid axons (Loligo Pealei) dialyzed with solutions free of ATP, and containing low physiological $[Ca^{++}]_i$ (0.02-0.04 μM), show a residual Ca efflux of about 2 $fmol.cm^{-2}.s^{-1}$(f/CS) that is not modified by the removal of Na_i or Na_o and Ca_o. Under these conditions and in the absence of Na_o and Ca_o, ATP activates Ca efflux with a very high affinity (Apparent K_{ATP} = 25 μM). Addition of Na_o and Ca_o causes only a small increment in Ca efflux. This ATP dependent, Na-Ca independent component, saturates to a value of about 175 f/CS at 0.5 μM $[Ca^{++}]_i$ (Apparent K_{Ca} = 0.18 μM). In the absence of ATP and at higher $[Ca^{++}]_i$, Ca efflux was found to be progresively more sensitive to Na_i, Na_o and Ca_o. (Apparent K'_{Ca} = 10 μM). Although ATP was not found to be essential for this component, it activates the Na-Ca dependent fraction with low affinity (Apparent K'_{ATP} = 220 μM). At very high $[Ca^{++}]_i$ (100 μM) most of the total Ca efflux depends on Na_o and Ca_o. The results presented here shows that the total Ca efflux can be divided in three main components: ATP dependent Na-Ca independent ('uncoupled pump'), Na-Ca dependent (Na/Ca exchange) and residual efflux (Leak). The marked different sensitivity between the first two components, toward ATP and Ca_i suggests the presence of two different mechanisms for Ca transport. The first component ('uncoupled') appears to be the most relevant for Ca extrusion at physiological pCa.

Supported by grant BNS 76-81050 from the US NSF to L.A.B.

W-AM-C2 CYANIDE SENSITIVE CALCIUM BUFFERING IN INTACT SQUID AXONS. F.J. Brinley, Jr., and J. Teresa Tiffert. Dept. of Physiology, University of Maryland School of Medicine, Baltimore, Md. 21201.

Free calcium concentration was monitored in axoplasm of isolated squid axons by use of microinjected arsenazo III or antipyrylazo III in conjunction with multiwavelength differential spectroscopy. The calcium load imposed upon fibers either by soaking or stimulation in 112 mM calcium saline was estimated from published analytical data on comparably treated axons. Increase of free calcium produced by CN pulses (5-15 s. exposure to 0.5-2 mM CN), calculated from measured absorbance changes and in vitro calibrations, was taken as a measure of the CN sensitivity of axoplasmic calcium buffers. The ATP content of the fibers (2.6 mM) was unaffected by CN pulses or stimulation at 100 pulses/s for 60 minutes. Fibers exhibited little or no sensitivity to CN pulses during soaks in 112 Ca saline but evidenced a progressive increase in sensitivity during prolonged stimulation (∿60 min.), a procedure which loads axoplasm with calcium at about 50 μM/min. After stimulation fibers were bathed in 0 Ca 0 Na saline to minimize loss of the imposed load. The sensitivity of Ca sequestration to CN pulses under these conditions disappeared with a half time of about 12 minutes. Microinjection of apyrase which reduced ATP to 100-150 μM did not affect buffering during prolonged stimulation nor sensitivity to CN pulses. However, the half time of loss of CN-pulse sensitivity after stimulation was increased 2 fold. These results confirmed earlier studies indicating that Ca buffering requires respiration but not ATP, and further suggest that heavy Ca loading marginally depletes a critical respiration dependent energy state. Supported by PCN 77-03916, BNS 76-19728-A01, NS 13420-03.

W-AM-C3 Ca MEASUREMENT IN THE PERIPHERY OF AN AXON. L. J. Mullins and J. Requena. Department of Biophysics, University of Maryland School of Medicine, Baltimore, Maryland, and Centro Biofisica y Bioquimica, IVIC, Caracas.

Aequorin has been microinjected into squid giant axons, the axons stimulated and the change in light emission followed. This response has been compared with that found when the axon, in addition to being microinjected with aequorin, is also injected with large concentrations of phenol red. This introduction of phenol red into axons results in a high probability that photons emitted by aequorin when it reacts with Ca in the core of the axoplasm, will be absorbed before they escape from the axon; photons produced by the aequorin reaction at the periphery of the axoplasm are much less likely to be absorbed. This technique thus favors observing changes in Ca_i taking place in the periphery of the axon. Stimulation in 50 mM Ca seawater of an aequorin-phenol red injected axon at 180 s^{-1} for 1 min produces a scarcely detectable change in Ca_i; the addition of 2 mM CN to the seawater produces an easily measureable increase in Ca_i suggesting that mitochondrial buffering in the periphery is substantial. Making the pH of the axoplasm alkaline either with 30 mM NH_4^+ - 50 mM Ca seawater, or by microinjecting 1 M KTES pH 8, reduces the resting glow of the axon but results in an even more substantial increase in Ca_i with stimulation.

Aided by grants (BNS-76-19728-A01, PCM 76-17364, NS-13402, and CONCIT 3126-S1-0602).

W-AM-C4 BUFFERING OF INTERNAL H^+ IN NEURONS. Z. Ahmed & J. A. Connor, Dept. of Physiol. & Biophys., Univ. of Ill., Urbana, Ill. 61801.

Intracellular buffering of H^+ was measured in neurons from the marine gastropod, Archidoris monteryensis using three different experimental protocols. I. HCl or H_2SO_4 mixed with $Na_2{}^{35}SO_4$ in measured ratios was pressure-injected into single neurons and the resulting pH change determined from the absorbance change of intracellular phenol red. The quantity of H^+ injected was determined from cellular ^{35}S content. Two distinct populations of identifiable neurons with respect to H^+ buffering were noted with capacities ($B.C._{cell}$) of 4.0 to 6.0 mEq/unit pH and 15.0 to 25.0 mEq/unit pH. II. Ca^{++} influx during spike activity or voltage clamp pulses causes an intracellular pH decrease (Connor & Ahmed, Biophys. J. 21: 186a, 1978). Cells were injected with measured amounts of MOPS buffer (pH 7.2) to reduce this intrinsic pH change (ΔpH_i) to a new level (ΔpH_m). Then, using the in vitro buffering capacity of MOPS under approximately intracellular ionic conditions ($B.C._{MOPS}$) and the expression $B.C._{cell} = B.C._{MOPS}/(\Delta pH_i/\Delta pH_m - 1)$, the $B.C._{cell}$ was determined. Values were 3.0 to 5.0 and 15.0 to 20.0 mM H^+/unit ΔpH. III. Neurons injected with measured amounts of EGTA were subjected to voltage clamp pulses of 1 to 4.0 sec. duration. The resulting Ca^{++} influx liberated H^+ intracellularly. Total calcium entry was determined from V-clamp current, and the stoichiometry of the partial reaction, EGTA + $Ca^{++} \rightleftarrows$ CaEGTA + nH^+ was estimated from in vitro measurements. Cell buffering capacity at this rapid time scale was computed after correcting for EGTA buffering capacity. This method did not show the differences between neurons as did I and II. For cells injected with EGTA at concentrations up to 3.0 mM, the $B.C._{cell}$ values were between 10 to 30 mEq/unit pH.

Supported by NSF-19938 and PHS RR-07030.

W-AM-C5 INTRACELLULAR CALCIUM REGULATION BY MOLLUSCAN NEURONS. J.A. Connor & Z. Ahmed (Intr. by J.L. Rabovsky) Dept. of Physiol. & Biophys., Univ. of Ill., Urbana, Ill. 61801.

The indicator dye Arsenazo III, microinjected into neural somata from the marine gastropod, Archidoris monteryensis, was used to monitor the decline of internal free calcium concentration following a voltage clamp pulse or action potentials. Under normal conditions the time course over which $[Ca^{++}]_i$ is restored to resting level has two components: a rapid one, which begins within 500 msec of the loading pulse onset and contributes significantly to the time course for 3 to 5 sec, and a slow component whose duration generally runs tens of seconds at 12°C. FCCP or CN^- had little effect on the fast component but extended the time course of the slow component. Injection of a mixture of apyrase and oligomycin had an effect similar to FCCP. Complete replacement of $[Na^+]_o$ by either TMA, choline or Li^+ also extended the slow phase time course. Sodium replacement following either FCCP treatment or injection of apyrase + oligomycin gave a greater reduction in the Ca^{++} uptake rate than either treatment alone, but still did not alter the fast phase noticeably. Injection of cAMP or exposure to saline containing IBMX (2.5 mM) slightly changed the rapid phase and produced an overall slowing of Ca^{++} uptake, but one which was much smaller than that observed with FCCP or 0 Na^+. Exposure to NH_4Cl (10 mM), which increases the intracellular pH, did not affect the Ca^{++} uptake time course, but internal acidification with CO_2, slowed the uptake of Ca^{++}. Internal acidification and alkalinization caused an increase and decrease in the resting $[Ca^{++}]_i$, respectively. Results indicate that at physiological loads of Ca^{++}, mitochondria and Na^+-Ca^{++} exchange may have an important role in regulating intracellular Ca^{++}, but are not the only important systems.

Supported by NSF-19938 and PHS RR-07030.

W-AM-C6 EFFECTS OF EXTERNAL Ca^{2+} ON VOLTAGE DEPENDENT CHANGES IN INTERNAL Ca^{2+} CONCENTRATION INVESTIGATED WITH ARSENAZO III. A.L.F. Gorman and M.V. Thomas*, Dept. of Physiology, Boston U. Sch. of Med., Boston, MA. 02118.

Changes in free intracellular Ca^{2+}, $[Ca]_i$, were measured with arsenazo III during depolarizations of the voltage clamped Aplysia neuron R-15 in different external Ca^{2+} concentrations and in the presence of different external divalent ions. In normal ASW (10 mM Ca^{2+}) depolarizations (10 to 1000 ms) from a holding potential of -50 mV cause an increase in absorbance, signifying an increase in $[Ca]_i$, which persists throughout the length of the pulse. Beyond about -20 mV the absorbance increases steeply with membrane depolarization, reaches a maximum at about +30 to +40 mV and declines at higher voltages. Suppression of the absorbance change occurs at potentials greater than about +150 mV. The change in absorbance is dependent on pulse duration, but typically $[Ca]_i$ increases about 500 nM at the peak of the absorbance curve produced by 300 ms depolarizations. Absorbsance changes are abolished by the addition of La^{3+}, Cd (>1mM) or Ni^{2+} (>5mM) to normal ASW or by Ca^{2+} free ASW, but are unaffected by TTX. The absorbance curve versus external Ca^{2+} concentration saturates at higher concentrations. Saturation is more apparent at potentials below 0 mV and less apparent at more positive potentials. Lowering external Ca^{2+} from normal values causes a negative shift in the peak of the $[Ca]_i$/voltage relation. The absorbance changes in different external Ca^{2+} can be predicted by an adsorption isotherm where the disassociation constant (K_{Ca}) and the maximum absorbance are voltage dependent. Typically, K_{Ca} increases by about 20 mV/e-fold change in potential between -20 to +60 mV. Supported by NS 11429.

W-AM-C7 VOLTAGE DEPENDENCE OF THE Ca^{2+} ACTIVATED OUTWARD CURRENT IN MOLLUSCAN NEURONS INVESTIGATED WITH ARSENAZO III. M.V. Thomas* & A.L.F. Gorman (Intr. by W. Lehman), Dept. of Physiology, Boston U. Sch. of Med., Boston, Mass. 02118

Changes in free intracellular Ca^{2+} were measured with arsenazo III during step depolarizations of membrane potential in the voltage clamped Aplysia neuron R-15 and compared to changes in membrane outward current. Brief (100-300 ms) depolarizations from a holding potential of -50 mV cause an increase in dye absorbance, signifying an increase in $[Ca]_i$, which persists throughout the pulse. In normal ASW (10 mM Ca^{2+}) the absorbance change increases steeply with membrane depolarizations beyond -20 mV, reaches a maximum at about +30 to +40 mV and declines at higher voltages. Suppression of the absorbance change occurs at potentials greater than +150 mV. In normal ASW the current voltage relation is N shaped. Membrane outward current increases steeply with step depolarizations with an initial maximum at about +50 to +70 mV and a minimum at +100 to +120 mV beyond which it again increases. In Ca^{2+} free ASW all absorbance changes at positive membrane potentials are abolished and the N shape of the IV relation is significantly reduced. The difference current (ΔI) obtained by subtraction of the total outward current in Ca-free ASW from that in normal ASW is assumed to represent the Ca^{2+} activated K^+ current. The shape of the difference current versus membrane potential is similar to that for the absorbance curve. Both start and are suppressed at similar potentials. The maximum of the difference current, however, is typically 20 to 30 mV more positive than the absorbance curve maximum. A similar displacement (10 to 20 mV) is found if the difference in membrane conductance (ΔG) is plotted in place of ΔI. This shift in conductance on the potential axis with respect to absorbance can be accounted for if the K^+ channels activated by an increase in internal Ca^{2+} are voltage dependepnt. Supported by NS 11429.

W-AM-C8 INTRACELLULAR DIVALENT CATIONS AND POTASSIUM PERMEABILITY IN MOLLUSCAN NEURONS. A. Hermann* and A.L.F. Gorman, (Intr. by J. Head), Boston U. Sch. of Med., Dept. of Physiology, Boston, MA., 02118.

Electrophoretic injection of Ca^{2+} into voltage clamped Aplysia neurons activates an outward current carried primarily by K^+ ions. The magnitude of this current is determined by the intensity and duration of the injection current, the position of the injection electrode within the cell and the holding potential. The efflux of K^+ ions measured with an extracellular K^+ sensitive electrode is a linear function of the Ca^{2+} activated outward current and disappears at its reversal potential. The outward current decays exponentially with an early time constant of 7 sec. and a late time constant of 27 sec. The early but not the late phase is temperature dependent with a Q_{10} of 3.4. If Ca^{2+} exerts its effect by interacting with a site on the inner surface that controls the conductance of the membrane to K^+ ions, then it should be possible to probe the specificity of this site by using a number of divalent cations of different ionic radius. Our results show that the order of affinity of divalent cations for activation of the K^+ current is $Ca^{2+}>>Hg^{2+}>Sr^{2+}>Mn^{2+}>Fe^{2+}$. Other divalent ions ($Ba^{2+}$, Cd^{2+}, Co^{2+}, Cu^{2+}, Mg^{2+}, Ni^{2+} and Zn^{2+}) are ineffective. After prolonged Cd^{2+} injection, the outward current activated by Ca^{2+} is increased 5 to 6 fold, whereas after a prolonged Ca^{2+} injection it is reduced. Prolonged injection of Ba^{2+} inhibits all currents carried by K^+ ions. It is concluded that the effectiveness of a divalent cation in activating the potassium current is, in part, related to its ionic radius. With the exception of Cd^{2+}, the site of activation can accommodate ionic radii between 0.76 Å to 1.30 Å. Supported by NS 11429 .

W-AM-C9 CALCIUM CHANNEL INACTIVATION IN SYNAPTOSOMES D.A. Nachshen (Spon: M.P. Blaustein) Dept. Physiol. and Biophys., Washington Univ. Med. Sch., St. Louis, MO. 63110

The time course of ^{45}Ca uptake was examined in pinched-off nerve terminals (synaptosomes) from rat brain. ^{45}Ca uptake was measured in synaptosomes incubated in media containing 20 μM Ca and either low (5 mM) or high (77 mM) potassium. The K-stimulated (depolarization-induced) Ca uptake appears to be mediated by voltage-sensitive Ca channels (cf. Blaustein, J. Physiol. 247: 617, 1975) that are blocked by Mg, Co and Ni. The K-stimulated ^{45}Ca uptake has an initial, rapid phase which is complete within one sec; this is followed by a slower phase which proceeds at a constant rate for about 20 sec. At longer times, the rate of uptake declines. The Q_{10} for the K-stimulated Ca uptake during both the initial rapid phase, and the slower phase has a value of about 2. The two phases of uptake have a similar Ca dependence: uptake saturates at high Ca concentrations, and the apparent half-saturation concentration (K_{Ca}) is about 150 μM. The initial, rapid phase of ^{45}Ca uptake is abolished by preincubating the synaptosomes in high-K solution either in the presence, or absence of external Ca. The later phase of ^{45}Ca uptake is unaffected by preincubation in high-K media. The data suggest that Ca uptake into synaptosomes is mediated by voltage-sensitive Ca channels, and that the decrease in the rate of Ca uptake seen after one second is due to inactivation of some of the channels. Supported by NIH grant NS-08442 to M.P. Blaustein.

W-AM-C10 INTRACELLULAR CHANGES OF H^+ AND Ca^{2+} ACTIVITIES IN APLYSIA NEURONS. J.D. Owen and H. Mack Brown. Department of Physiology, University of Utah, Salt Lake City, Utah, 84108.

pH and Ca^{2+}-selective microelectrodes (Thomas, J. Physiol. 238: 159-180, 1974; Brown, Pemberton & Owen, Anal. Chim. Acta 85: 261-276, 1976, respectively) were used to measure intracellular changes in H^+ and Ca^{2+} activities in Aplysia giant neurons. While the cell was bathed with a pH 7.65 artificial seawater (ASW) solution, the intracellular pH, pH_i was 7.25. Upon stimulation with 5% bubbled ASW, pH_i fell to 6.95, which corresponds to a buffer power, β, for the cell of 43 mM HCO_3^-/pH unit. Long white light flashes had no effect on pH_i or the intracellular calcium ion activity (a^i_{Ca}). Also, 5% CO_2 or sustained activation had no effect on a^i_{Ca}. a^i_{Ca} was increased from 8.2×10^{-6}M to $1.4^2 \times 10^{-3}$M by pressure injecting 100 mM $CaCl_2$ with 60 psi of N_2 for 50 sec through a 1.5 µm tip diameter electrode. The rate of the $^2Ca^{2+}$ removal was found to be 17.2 pmole · cm^{-2} · sec^{-1}. During the pressure injection of Ca^{2+}, V_m depolarized slightly while a^i_{Ca} increased dramatically. After the pressure was turned off, a^i_{Ca} continued to increase slightly and then decrease, while V_m hyperpolarized and then returned to its resting V_m. The time course for the maximum increase in a^i_{Ca} and V_m hyperpolarization were different, with the a^i_{Ca} peak preceeding the V_m peak by about 30 sec. This work was supported in part by grants (EY 02402 and EY 00762) from the National Eye Institute.

W-AM-C11 INTRACELLULAR Ca^{2+} ACTIVITY IN BALANUS PHOTORECEPTORS MONITORED WITH Ca^{2+} SENSITIVE MICROELECTRODES. H. Mack Brown and J.D. Owen, Department of Physiology, University of Utah, Salt Lake City, Utah, 84108.

Intracellular Ca activity was monitored with Ca^{2+} sensitive microelectrodes as described by Brown, Pemberton and Owen (Anal. Chim. Acta 85: 261-276, 1976). Membrane potential was simultaneously monitored with an intracellular KCl-filled microelectrode. Resting intracellular Ca activity of dark adapted cells ranged between 1×10^{-7} and 1×10^{-6}M Ca^{2+}. The V_{Ca} of the Ca electrode did not change upon illumination of the cell, nor was there any indication that a^i_{Ca} was altered during the time shortly after illumination was extinguished. Caffeine reduced the steady state level of the receptor potential during illumination but there was no evidence of an increase in a^i_{Ca}. Total block of the receptor potential produced by 10 mM ruthenium red was not associated an immediate change in a^i_{Ca} although there was an increase recorded 5-10 min after the receptor potential was blocked. These results indicate that Ca^{2+} is very well buffered in these cells and does not increase above the micromolar level with illumination. However, if the true intracellular Ca activity is but a few nanomolar and if there is high levels of Mg^{2+} in these cells, very small changes (submicromolar) in a^i_{Ca} would be beyond the resolution of the present experimental techniques. This work was supported in part by grants (EY 00762 and EY 02402) from the National Eye Institute.

W-AM-C12 LIGHT-INDUCED PH CHANGES MEASURED BY DOUBLE-BARRELED PH MICROELECTRODES IN BALANUS PHOTORECEPTORS. J. Coles,* S. Levy* and A. Mauro. Department of Physiology, University of Geneva School of Medicine, Geneva, Switzerland and Rockefeller University, New York, N.Y.

In the course of establishing whether pH changes are associated with anoxia in invertebrate photoreceptors it was observed that a steady light alone induced an increase in the internal pH (pH_i) of photoreceptor cells in lateral ocelli of Balanus eburneus. In 8 cells pH_i increased on average by 0.2 pH units. In a previous study Brown and Meech [J. Physiol. (Lond.) 1976, 263:218P] have reported that pH_i decreased by 0.1 to 0.2 pH units with steady light. It is not clear how these contradictory results can be explained. It may be relevant to note that Meech and Brown used a Thomas-type pH microelectrode which consists of a recessed H^+-sensitive glass membrane fused to the tip of a micropipette about 1µm in diameter. A second conventional micropipette serves as an intracellular reference electrode. In our study we have used a Carter-type pH microelectrode. A double-barreled micropipette is pulled from θ glass to a diameter of about 4 µm, beveled and, by heating, sealed with an H^+-sensitive glass membrane. Rupturing the membrane of one barrel by applying a 50-volt pulse provides a "local" reference electrode while the remaining sealed barrel serves as a pH electrode. Data will be presented showing the potentials recorded between an extracellular reference electrode and the pH electrode, and the intracellular("local")reference electrode, respectively. Subtracting the photoreceptor potential common to both recordings yields the pH electrode potential. By injecting a common mode signal in series with the extracellular reference electrode and ground, rejection of the common mode response was checked and adjustments were made when necessary before each pH_i recording. This procedure virtually eliminated any common mode artifact in the pH_i recordings.

W-AM-C13 LIMULUS PHOTORECEPTORS HAVE A TRANSIENT OUTWARD CURRENT NOT DEPENDENT ON Ca^{2+} ENTRY. J.E. Lisman, Brandeis U., Waltham, Mass., M.C. Swan and G.L. Fain UCLA, L.A.

Voltage-dependent currents were measured in the dark using a two microelectrode voltage-clamp technique with linear leakage correction. From a holding potential of -70mV, large depolarizing pulses evoked an outward current which decayed to a nearly steady value within 1 sec. at room temperature. This transient current could be inactivated by raising the holding potential from -70mV to -40mV. The transient and maintained components of outward current could be separated pharmacologically. The transient component was preferentially depressed by 1mM 4-aminopyridine. In contrast, the maintained component was preferentially depressed by intracellular injection of TEA. It was of interest to determine whether the transient outward current was activated by voltage-dependent Ca^{2+} entry. Small depolarizations evoke a net inward current. This current is probably carried in part by Ca^{2+} because the current was attenuated (50-75%) when Ca was removed from the seawater or Co^{2+} was added. Zero Ca^{2+} seawater with 10mM Ni^{2+} completely blocked the inward current but did not block the transient outward current. Therefore there is a transient component of outward current that is not activated by Ca^{++} entry. We conclude that ventral photoreceptors contain a rapidly inactivating voltage-dependent conductance which is different from the condutance that carries the maintained current. This transient outward current closely resembles a current found in molluscan neurons which has been called the A-current. This is, to our knowledge, the first description of an A-current outside the Phylum, Mollusca.

W-AM-C14 VOLTAGE DEPENDENCE OF CALCIUM AND POTASSIUM PHOTORECEPTOR CURRENTS DURING AND AFTER LIGHT STEPS. D. L. Alkon, NINCDS, NIH, MBL, Woods Hole, MA.

Under voltage clamp (with two microelectrodes) no voltage changes ($\geq$ 20 μV) were elicited by 30-sec light steps ($\geq 10^{3.5}$ ergs/cm^2-sec) from Type B photoreceptors (of the nudibranch Hermissenda). Light-elicited currents for cells with cut axons (i.e. without synapses or impulses) were comparable to those of intact cells. The first (inward) current, (probably Na^+), began $\sim$20 msec after light onset, reversed at $\sim$+50 mV and decreased $\sim$90% after replacing Na^+ in artificial seawater (ASW) with equimolar TMA. The second (outward) current (K^+) began $\sim$0.5 secs and peaked $\sim$2-4 secs after light onset. It decreased to $\sim$10% maximum 7-8 secs after light onset. This K^+ current reversed at $\sim$-75 mV was more apparent in TMA-ASW, and decreased in external (2-4 mM) 4-aminopyridine (4-AP), external Ni^{++} (1 mM), lowered external Ca^{++} (2.5 mM) with higher external Mg^{++} (65 mM), and after intracellular injection of TEA. This K^+ current was reduced in 30 mM external K^+ and was not observable in 60 mM K^+. A small (outward) current (late K^+) followed the light step and was similarly affected by these treatments except that it increased at +30 to +50 mV. A third (inward) current (Ca^{++}) began $\sim$0.5 sec after light onset and persisted for 1-2 mins after light steps. The Ca^{++} current reversal potential was > +85 mV. This current remained in 60 mM external K^+ and 4-AP, was reduced by external Ni^{++} (1 mM) and eliminated in 2.5 mM external Ca^{++} (with 65 mM Mg^{++}). The Ca^{++} current in TMA-ASW was not present at < +15 mV. (In TMA-ASW the residual Na^+-current reversal potential was $\sim$+15 mV). Persistent Type B depolarization ("LLD", Alkon & Grossman, J. Neurophys. 1978) after light, then, arises from increased Ca^{++} and decreased Ca^{++}-dependent-K^+ current. The potential dependence of these currents can explain the specificity of stimulus pairing (which causes more depolarization) necessary to an associative learning model (Alkon, J. Gen. Phys., 1975, 1975; Crow & Alkon, Science, 1978).

W-AM-D1 THE TIME COURSE OF ENERGY BALANCE IN AN ISOMETRIC TETANUS. E. Homsher, C. Kean, A. Wallner*, and V. Sarian*, Department of Physiology, U.C.L.A., Los Angeles, CA 90024.

Energy balance studies have shown that as much as 50% of the enthalpy produced during an isometric tetanus can not be explained by ATP or phosphoryl creatine (PC) dephosphorylation and indicate the presence of additional exothermic reaction (s). To characterize these unknown reactions, the time course of the unexplained enthalpy production was measured in isometric tetani of Rana temporaria sartorius muscles at l_o and 0°C. The total enthalpy production and the amount of ATP and PC split was measured in tetani lasting 0.75, 1.5, 3, 5, 6, 8, 13, 15, and 20 seconds. The unexplained enthalpy produced at each time point was taken as the difference between the observed enthalpy and that accounted for by the measured ATP and PC splitting. The results of these experiments showed that: 1) it is only during the first 8 seconds of a tetanus that unexplained enthalpy is produced; all subsequent enthalpy production can be explained by the measured PC splitting; 2) the rate of unexplained enthalpy production, which is most rapid at the start of a tetanus, declines progressively and approaches zero by 8 seconds; 3) the total amount of unexplained enthalpy produced in a tetanus lasting 8 seconds or longer is 45.9 ± 7.4 mJ/g of muscle. The results suggest that the unexplained reactions are associated with the calcium release-reaccumulation mechanism, and not with the cross bridge mechanism.

(Supported by USPHS grants # HL 11351 and AM 70792 and AHA-GLA grant #525.)

W-AM-D2 MAMMALIAN SMOOTH MUSCLE: ECONOMICAL, BUT INEFFICIENT. T.M. Butler, M.J. Siegman, and S.U. Mooers* Department of Physiology, Thomas Jefferson Univ., Philadelphia, PA 19107.

Rabbit taenia coli muscles were treated with metabolic inhibitors to stop glycolysis and respiration and were subjected to one of the following at 18°C: [A] stimulation (60 Hz, AC) for 35 sec at 105% l_o; [B] stimulation for 35 sec while shortening from 105% l_o to 88% l_o at a constant velocity ($4.8 \times 10^{-3} l_o$/sec); [C] unstimulated control. ATP and phosphocreatine were measured and normalized to total creatine content, Ct = 2.7 μmole/g. There was no significant difference in the chemical energy usage during the isovelocity and isometric contractions. In design B, the active external work produced per mole of high energy phosphate utilized was 5.2 ± 1.1 kJ/mole, N = 7, and is 3-5 times lower than that obtained in similar experiments on striated muscle. The low external work output per mole ~P was not due to possible deleterious effects of the metabolic inhibitors since a similar experiment on untreated muscles gave a value of 6.2 ± 1.4 kJ/mole, N = 9. In another design, paired muscles were either [D] stimulated isometrically at 105% l_o for 20 sec or [E] treated as in D followed by continued stimulation while shortening to 88% l_o. The active external work produced during the shortening was 4.5 ± 1.3 kJ per mole of high energy phosphate utilized. At this velocity, the average active force during shortening was 0.4 P_o and similar values of work/Δ~P were obtained at velocities giving average forces of 0.3 and 0.7 P_o. The average rate of chemical energy utilization during shortening (E-D = -0.0064 ± 0.0008 mole/mole Ct·sec, N = 14) is significantly greater ($P<0.01$) than that observed previously for maintenance of constant isometric force (-0.0028 ± 0.0008, N = 18). This is a direct demonstration of the Fenn effect in smooth muscle. Although it is well known that smooth muscle is very economical at maintaining isometric force, we conclude that it is inefficient at active external work production. (Supported by 1S07 RR-05414 and HL 15835 to the Pennsylvania Muscle Institute)

W-AM-D3 THE DISSOCIATION OF MYOSIN FROM ACTIN BY ATP IN A CONTRACTING MUSCLE FIBER.

R. Cooke and W. Bialek*, Dept. of Biochem/Biophys. and the CVRI, University of California, San Francisco, CA 94143.

We have measured force-velocity curves for glycerinated rabbit fibers as a function of the ATP concentration. The maximum contraction velocity is proportional to [ATP] up to 1 mM ATP. We have used these data to construct models of the dissociation of myosin from actin. We have assumed that ATP binds and dissociates the myosin head before it begins to exert a negative tension (i.e., a tension that opposes contraction). This model correctly predicts the observed force-velocity curves for a wide range of ATP concentrations. The fit to the data requires that a) the rate constant for the binding of ATP to myosin is large, $\sim 10^5\ M^{-1}s^{-1}$; b) the work required to dissociate a head that does not bind ATP is 1.25 times greater than the maximum work which can be performed in a power stroke; and c) the force produced by a myosin head during a power stroke is independent of the velocity of contraction (at least up to 0.5 lengths/sec.). In the first model put forward to explain muscle contraction by A.F. Huxley in 1957, dissociation occurs mainly in a region in which the myosin head is exerting a negative tension. Setting the rate of actin-myosin dissociation proportional to [ATP] in this model produces force-velocity curves that do not have the observed shape. In general, models in which ATP binding occurs in a region of negative tension will not explain the data.

Work supported by grants from NSF BMS75-14793, AHA 78-845, and USPHS AM00479.

W-AM-D4 MECHANICS OF THE SINGLE CELL LAYERED HEART OF "SEA POTATO." L. Cleemann*, S. Dillon*, and M. Morad. MDIBL, Salisbury Cove, ME and Departments of Physiology, University of Pennsylvania, Philadelphia, PA 19104.

The single cell layered heart of Boltenia Ovifera consists of a straight tube propelling blood by peristaltic contraction. A segment of the myocardial wall was servo-controlled mechanically. The sarcomere length was measured by monitoring the position of the first order laser diffraction peak with a time resolution of a few msec. The passive pressure was small at sarcomere length below 2 μ but increases steeply with further stretch. During stimulated twitches the sarcomeres of the length clamped preparation shortened about .1-.2 μ simultaneous with broadening of the diffraction peak. The active twitch pressure increases linearly from 1.6 μ to about 2.1 μ and falls linearly with further stretches approaching zero at 2.4 μ. The length-tension relation did not have a prominent plateau. The twitch pressure reaches maximum in .3-.5 sec, complete relaxation requires 1-3 sec. The sarcomere shortening occurs mainly during the early part of the twitch (.2 μ in 40 msec) and is followed by an increase in the distribution of sarcomere lengths. Stretch and release experiments showed that transient responses were limited to the first 50 msec of length change, thereafter the twitch wave forms were similar. The results obtained with a small segment of the myocardial wall were compared to those in the intact heart. The wave of contraction was monitored on movie film and the luminal pressure at both ends of the heart recorded. A computer simulation relating the "small segment parameters" to the performance of the entire heart is described. (HL 17702).

W-AM-D5 EFFECTS OF DIETHYL ETHER ON FUNCTIONALLY SKINNED MYOCARDIAL CELLS. J.Y. Su and W.G.L. Kerrick, Univ. of Wash., Sch. of Med., Seattle, WA., 98195

Diethyl ether, at clinical concentrations, directly depresses myocardial contractility(1). In order to better characterize diethyl ether-induced myocardial depression, we examined separately the effect on the contractile proteins and sarcoplasmic reticulum of functionally skinned rabbit myocardial cells. Right ventricular papillary muscle fiber bundles were mounted on tension transducers and immersed into control and test ether solutions of various [Ca^{2+}] and [EGTA]. Our techniques for studying the tension vs pCa relationship and for generation of 25 mM caffeine-induced tension transients have been described previously(2,3). The partial pressure (expressed as % of 1 atmosphere) of diethyl ether in the bathing solutions was assayed by gas chromatography. We found that diethyl ether, at 4 and 6% increased slightly the submaximum Ca^{2+}-activated tensions and caused a small decrease in the maximum tensions (pCa 3.8). We also found that diethyl ether increased 25 mM caffeine-induced tension transients when administered only during the Ca^{2+} uptake phase and decreased caffeine-induced tension transients when administered only during the Ca^{2+} release phase. The responses observed in each case were reversible. We conclude that diethyl ether increases Ca^{2+} uptake into and inhibits Ca^{2+} release from sarcoplasmic reticulum. Myocardial depression may, in part, be due to an inhibition of Ca^{2+} release from the sarcoplasmic reticulum. (Supported by grants from NIH HL 20754 and the Pharmaceutical Manufacturers Association Research Starter grant).

(1) Brown, B.R. & Crout, J.R., Anesthesiology 34:236(1971)
(2) Su, J.Y. & Kerrick, W.G.L., Pflugers Arch. 375:111(1978)
(3) Su, J.Y. & Kerrick, W.G.L., Biophy. J. 21:87a(1978)

W-AM-D6 EFFECT OF ATP BUFFER CONCENTRATION ON THE MECHANICAL RATE CONSTANTS IN CHEMICALLY SKINNED RABBIT PSOAS FIBERS. M. Kawai and P.W. Brandt. Depts. of Neurology and Anatomy, Columbia University, 630W 168th st, New York, N.Y. 10032

We reported earlier (Kawai, 1978: Biophys. J. 22,97) that the rate constants of oscillatory work ($2\pi c$) and high frequency exponential advance ($2\pi b$) follow Michaelis-Menten kinetics as MgATP (substrate) concentration is increased up to 20mM ($K_M \sim 1$mM; Figure). We can use this substrate concentration dependence to test the adequacy of any given concentration of an ATP regenerating system. If the ATP concentration in the core of the fiber falls below that in the bulk of saline, the observed rate constants will be smaller than the predicted values. Our standard conditions are (in mM of the Na salts) 1 MgATP, 2.8 CaATP, 5 free ATP, 7.5 phosphate, 43 propionate, 13 sulfate, 6 imidazole, 15 CP, 71 unit/ml CPK, pH 7.00, pCa 4.0, 20°C. In the experiments to be reported in which the substrate and its buffer system was varied, both ionic strength and Na concentration were kept constant. Marked slowing of the rate constants (to about half) below the predicted values were obtained in solution of 1 substrate, 1 free ATP, and either no CP nor CPK, but the deviation was eliminated, or less than 10%, if both 10 CP and 40 unit/ml of CPK were added. Intermediate slowing was observed between these two conditions. Addition of 1 to 10mM free ATP to the well buffered solution had no effect nor did addition of up to 16mM of creatine. Supported by grants from NSF PCM 78-08592, NIH NS 05910, NS 11766 & MDAA.

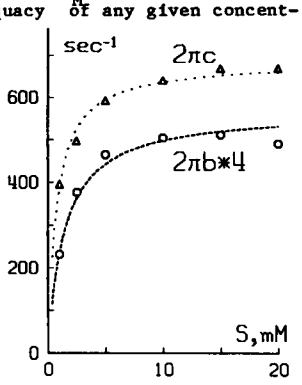

W-AM-D7 FAST RESPONSE OF CARDIAC MUSCLE TO QUICK LENGTH CHANGES. M. Delay, D. Vassallo*, T. Iwazumi and G. Pollack, University of Washington, Seattle, Wa 98195.

An apparatus has been developed which is capable of measuring the fast tension response to quick changes in sarcomere length. The technique, based on laser diffraction by muscle, allows measurement of sarcomere length every 0.2 msec; muscle length changes are complete in 0.25 msec; and tension is measured with a transducer with a response frequency of over 3 kHz. Measurements were made on very uniform regions of rat ventricular preparations. These regions were ∿ 0.6 mm long, compared to the 0.06 mm diameter of the laser beam. Muscle length changes were imposed upon the preparation, and the resulting changes in sarcomere length were computed by averaging the sarcomere length behavior over the uniform region. It was found that between 6 and 8 nm shortening per half sarcomere (about 0.6% of resting sarcomere length) is required to drop the tension to zero. Within experimental error, this value is equal to the corresponding figure for skeletal muscle. The decrease in muscle length needed to give the same result is between 2% and 3%, in agreement with previous experiments, and illustrates the effects of compliance of the end regions which are damaged by being mechanically clamped. Tension change is linear with sarcomere length change for releases, and for stretches of up to 12 nm per half sarcomere. The high compliance of the clamped ends implies that stretching them to develop substantial post-release tension might take on the order of 10 msec, thus masking the fast phases of tension recovery seen in skeletal muscle.

W-AM-D8 MEASUREMENT OF STIFFNESS DURING FAST TENSION TRANSIENTS IN FROG SKELETAL MUSCLE FIBRES. D.L. Morgan and F.J. Julian, Department of Muscle Research, Boston Biomedical Research Institute, Boston, MA 02114.

Several explanations have been proposed for the fast tension transients following sudden shortening of active frog single fibres. One potential method of distinguishing between these models is measurement of stiffness during the release and fast recovery phase. In the present experiments, small high frequency vibrations were used as a convenient method of measuring the stiffness of tetanically stimulated single twitch fibres from the anterior tibial muscles of Rana temporaria. The sinusoidal movement was superimposed on shortening steps of a range of sizes, up to those large enough to drop the tension almost to zero. Electronic subtraction of records without vibration from equivalent records with vibration was used both as a check that vibration had not significantly affected the response to the step, and to enable accurate estimation of stiffness on a cycle to cycle basis substantially free from the difficulties and uncertainties inherent when measuring a sinusoid superimposed on a rapidly changing baseline. Releases were completed in 0.5 msec and vibration frequencies ranged from 2 to 10 kHz. Results showed a small decrease in stiffness during the release, and a small increase in stiffness during the fast recovery of tension. When stiffness and tension were normalized to pre-release values, the stiffness changes were always less than one quarter of the tension changes. At no time did the stiffness exceed that prior to the release. The use of different frequencies did not significantly change the results. These experiments support models in which the fast recovery is ascribed principally to changes in state of existing cross-bridges, rather than attachment of new cross-bridges or detachment of compressed bridges. (Supported by USPHS HL-16606, AHA 77-616 and MDA.)

W-AM-D9 SARCOMERE LENGTH - ISOMETRIC TENSION RELATIONSHIP OF UNIFORMLY CONTRACTING SKINNED MUSCLE FIBERS. T. Iwazumi and G.H. Pollack, Univ. of Washington, Seattle, WA 98195

A slow activation method has been developed which permits full activation of skinned muscle fibers while retaining clear striations. This method has made it possible to reliably measure the sarcomere length (SL) during contraction by microscopy and diffractometry.

We used mechanically skinned rabbit soleus fibers, and all experiments were performed at 23°C. The protocol was to perform a sequence of contractions at average SL of 2.2, 2.7, and 3.2 μm using either "low Ca^{++}" (pCa=6) or "high Ca^{++}" (pCa=5) solutions. The order of the measurement cycle was 2.7-2.2-3.2-2.7 μm, and the tensions at the first 2.7 and the last 2.7 μm were required to match within 5% to ensure the repeatability. We measured the distribution of SL along the entire length of the fiber before, during, and after contraction, and the variation of the SL distribution in relaxation at any of these three lengths was required to lie within a band of 0.1 μm.

We have found that: 1) The repeatability of contractions is directly related to the uniformity of SL along the fiber. 2) The higher the tension and the longer the SL, the worse the uniformity during contraction; once the fiber has developed a large nonuniformity, it was irreversibly damaged. 3) The maximal stress that viable fibers can exert was very high; about 3 kg/cm^2. 4) The average SL (along the length) during contraction becomes slightly shorter than that of before contraction. 5) The SL-tension relationship thus measured has always a positive slope; the longer the SL, the greater the tension at either low or high Ca^{++}. Supported by AHA-75791 and NHLBI-18676. GHP is an Est. Investigator of AHA.

W-AM-D10 TENSION TRANSIENTS IN CALCIUM-ACTIVATED SKINNED FIBERS FROM ADULT PSOAS AND SOLEUS AND NEWBORN PSOAS MUSCLES OF THE RABBIT. R.L. Moss and F.J. Julian, Department of Muscle Research, Boston Biomedical Research Institute, Boston, MA 02114.

The tension responses of mammalian skinned skeletal muscle fibers to length steps, complete in about 0.7 ms, have been investigated. Psoas and soleus muscles were isolated from young male rabbits (about 3.5 kg) and psoas muscles from newborn rabbits (50-60 g). Small bundles of approximately 50 fibers were dissected from the muscles in skinning solution containing, in mM: K-proprionate, 180; EGTA, 5; ATP, 4; $MgCl_2$, 1; imidazole, 10 (see Wood, et al., Science, 187:1075, 1975). The fibers were stored in cold skinning solution for up to 3 days and were then placed in skinning solution containing Brij-58 (0.5%, W/V) for 1 hour before use. Fiber segments were mounted between a servo motor and force transducer, and segment length was adjusted to achieve a sarcomere length, measured through a microscope, of about 2.3 μm during maximal activation with calcium. The pCa of the activating solution was 5.49 and the temperature was 10°C. The tension transients recorded from the adult psoas fibers were similar in form to the T_1 and T_2 phases which have been observed previously in frog living twitch fibers. The extrapolated length change to reduce tension to zero was about 11.5 nm/half-sarcomere in each of the preparations; however, the amounts of rapid tension redevelopment in the adult soleus and newborn psoas muscles were much lower than in the adult psoas. In terms of, for example, the Huxley and Simmons model of contraction (Nature, 233:533, 1971), the results suggest that the instantaneous stiffness of the myosin S-2 parts of these muscles are similar. The observed differences in tension recovery suggest possible differences in the kinetics of cross-bridge head rotation. (Supported by USPHS HL-16606, AHA 77-616 and MDA.)

W-AM-D11 STEPWISE SARCOMERE SHORTENING: EFFECT OF LOAD AND TEMPERATURE ON PAUSE DURATIONS D.V. Vassallo* and G.H. Pollack, Univ. of Wash., Seattle, Wash., 98195

A series of afterloads was imposed on rat trabecular specimens contracting at 26°C. Sarcomere lengths were measured by laser diffraction, with time resolution at 200 μsec. As previously reported (Pollack et al., Nature 268: 757, 1977), sarcomere shortening occurred in stepwise fashion, with bursts of shortening punctuated by periods of zero velocity, hereafter referred to as "pauses."

We varied the afterload level and measured the pause durations at each afterload. At zero load the pause durations averaged 11.2 ± 4.7 msec (SEM; 7 experiments). At the highest load studied, 1.6 g/mm^2, the duration increased to 21.8 ± 3.5 msec. The relation between pause duration and load was approximately linear. During the initial portion of shortening, pause durations were independent of time; however, late in the shortening, around the expected time of onset of relaxation, pause durations increased exponentially with time; thus pause durations may increase as activation level diminishes toward the end of contraction.

The effect of temperature variation was studied in the range of 20° to 32°C. We used two protocols: first, the above protocol was repeated at several temperatures; and second, a particular pause was followed as the bath temperature was suddenly altered. In both protocols reduced temperatures resulted in increased pause durations. We do not have sufficient data to compute the value of Q_{10} reliably.

The results suggest that increased pause durations at the sarcomere level may account, at least in part, for the diminished muscle shortening velocity found under diverse conditions such as high loads, low temperatures, or reduced activation levels.

W-AM-D12 LENGTH DEPENDENT FORCE-VELOCITY RELATIONS IN CARDIAC MUSCLE SEGMENTS. L.L. Huntsman and D.S. Joseph*, Center for Bioengineering, University of Washington, Seattle, WA 98195.

The force-segment length (F-SL) and force-velocity (F-v) relations have been determined for central segments of isolated papillary muscles under both load clamp and auxotonic (muscle isometric) conditions. Muscle isometric contractions at various lengths show peak force to vary approximately linearly with SL with no evidence of the expected plateau at longer lengths. However, the trajectories of these contractions in the F-v plane show peak force to occur at non-zero velocities, suggesting that the measured peak force may not adequately indicate the potential for isometric force (F_{max}). Analysis of the F-v data allows estimation of F_{max} and V_{max} by extrapolation and their dependence on SL can then be assessed. The F-v data from the two protocols are in close agreement and form curves which are: a) adequately described by the Hill equation; b) time independent from ∿ 20msec to the time of peak force (∿ 250msec); c) independent of segment length (SL) above 0.85 SL_{max}; and d) depressed symmetrically in proportion to reductions of SL below 0.85 SL_{max}. The time independence suggests that mechanical activation is essentially constant over most of the rising phase of contraction. Estimating SL_{max} to be 2.35μ, F_{max} and V_{max} are seen to be independent of length above 2.0μ and fall linearly below that value, approaching zero around 1.65μ. No evidence of shortening-induced deactivation is apparent up to the time of peak force.

Supported in part by NIH grants HL 20613 and HL 00344, and by a Grant-in-Aid from the American Heart Association.

W-AM-E1 ATP DRIVEN PH GRADIENT IN RAT LIVER MITOCHONDRIA STUDIED BY ^{31}P NMR. S. Ogawa, C. Shen* and C.L. Castillo*, Bell Laboratories, Murray Hill, N.J., 07974.

^{31}P NMR has been used to study the increase of ΔpH in mitochondria by externally added ATP. Freshly prepared mitochondria were treated with NEM and well washed so as to inhibit the exchange between internal and external P_i. Upon addition of ATP(7mM), phosphocreatine(30mM) and creatine kinase to a NMR sample of mitochondria suspension (∿100mg protein/ml) at 0°C, a slight increase of ΔpH by ∿0.3pH unit was observed. However the increased ΔpH could not be maintained but slowly decayed along with the increase of external ADP/ATP ratio. Further addition of valinomycin to the suspension induced a large ΔpH(0.8) which was maintained by the increased rate of internal ATP hydrolysis as seen in the growth of the internal P_i peak intensity in NMR spectra and the concominant decrease of the external phosphocreatine peak. The external P_i and ATP peaks stayed virtually constant. When carboxyatrctyloside was added to inhibit the ATP/ADP translocator, the internal P_i increase was stopped and the ΔpH decayed. These observations in conjunction with those made earlier in respiring mitochondria clearly show the reversible nature of the ATPase function in which the internal ATP hydrolysis is associated with the outward pumping of protons. The present results also show that internal P_i is not directly involved in the process of the external ATP/int. ADP exchange.

W-AM-E2 ELECTRICAL RESISTANCES OF GIANT MITOCHONDRIA MEASURED WITH MICROELECTRODES. Charles Bowman and Henry Tedeschi, Dept. of Biological Sciences and the Neurobiology Research Center, The University at Albany, Albany, N.Y. 12222.

A study of membrane resistances was carried out with giant mitochondria isolated from the liver of mice kept on a diet containing cuprizone [see Maloff et al, J. Cell Biol. 78:199, 244 (1978)]. Two microelectrodes were used, one to deliver current pulses and the other to deliver current and/or record potentials simultaneously. The following results are apparent. (a) The resistances generally ranged from 1 to 4 MΩ. Assuming no convolutions in the surface membrane, the specific resistances ranged from 0.4Ωcm^2 to 5Ωcm^2. (b) The current pulses (10^{-10}amp) did not induce a potential when the microelectrodes were outside the mitochondria, even when in contact with the surface or in contact with each other. (c) In the cases in which there was no membrane potential, no potential could be induced by the current pulses. (d) When the current pulses were progressively increased in magnitude (from about 10^{-10}amp), the resistances irreversibly decreased, either gradually or over a narrow range of currents. (e) Very low current pulses (below 10^{-10}amp) revealed resistances in the same range as those measured with pulses of 10^{-10}amp. We interpret results (a) to (d) as additional evidence for the location of the microelectrodes in the inner mitochondrial space. Aided by grant GM 23789-01 of NIH.

W-AM-E3 ELECTRON TRANSPORT ACROSS PHOSPHOLIPID BILAYERS CATALYZED BY HEME. Jennifer A. Runquist* and Paul A. Loach, Northwestern University, Evanston, Illinois 60201.

We are initiating a series of studies of electron transport across P-lipid bilayers as an approach to better understanding the in vivo electron transport systems and energy coupling mechanisms. In the first of these studies we have prepared P-lipid vesicles (using soybean phospholipids) containing hemin dimethyl ester (HDME) at a concentration varied between approximately 1 heme per 2500 P-lipids and 1 heme per 100 P-lipids. The vesicles were formed under anaerobic conditions with 5% pyridine present (to protect the heme) by a standard method[1] in a solution containing 0.2 M $K_3Fe(CN)_6$. External ferricyanide and pyridine were removed by gel filtration on Sephadex G-25. Electron transport was then initiated by adding these vesicles anaerobically to a solution containing reduced indigotetrasulfonic acid (ITSA) and the rate of oxidation followed at 600nm. We have observed a greater than 25-fold increase in the rate (maximum rate observed ≅ 30 moles ITSA oxidized/min/mole HDME) of oxidation with vesicles containing HDME relative to control vesicles. The rate is linearly dependent on the concentration of HDME. Because the HDME concentration in the membrane is less than 10% of that of the dye oxidized, HDME presumably shuttles from one side of the membrane to the other as an electron carrier. Using a Pressman cell, we have also demonstrated that HDME catalyzes the transport of ^{14}C labelled SCN^- from an aqueous phase through a chloroform phase to a second aqueous phase. In this case the catalytic effect of HDME was 2500 times the control rate. Thus HDME can transport both electrons and anions (presumably in a coupled reaction).

1. A Modification from Hauska, G., FEBS Lett 79, 345 (1977).

W-AM-E4 OXIDATIVE PHOSPHORYLATION AND MEMBRANE PHASE TRANSITIONS IN RAT LIVER MITOCHONDRIA. H. Rottenberg, Hahnemann Medical College, Phila. PA 19102.

The temperature dependences of the rates of succinate oxidation, phosphorylation, ATPase activity and the formation of membrane potential in rat liver mitochondria were investigated in the range of 10-45°C. All processes show discontinuities in the range of 20°-30°C which confirm earlier suggestion that the mitochondrial inner membrane undergoes a phase transition in this temperature range. The acceptor respiratory control ratio (the stimulation of respiration during phosphorylation) the stimulation of respiration by uncouplers and ionophores and the stimulation of ATPase by uncouplers are maximal at 25°C dropping sharply at higher and lower temperatures. These data may indicate that the coupling is maximal within the phase transition. At 20°-30°C the large stimulation of respiration by ADP is associated with only a small reduction of membrane potential while a similar stimulation of respiration by potassium in the presence of excess valinomycin is associated with a much larger reduction of membrane potential as was previously observed by Padan and Rottenberg (1). These results were previously taken as indication for a direct coupling between oxidation and phosphorylation which is not mediated by proton current through the bulk phases. It is shown here that below and above the phase transition this discrepancy between ADP and valinomycin effect on respiration and membrane potential disappears. It is therefore suggested that the hypothetical direct coupling which is interpreted here as a direct proton current on the membrane surface, is maximized within the phase transition. It is possible that this effect is associated with protein clustering within the transition state. The chemiosmotic mechanism of oxidative phosphorylation in relation to the protonic current pathways is discussed and a role for phase transitions in the control of coupling in energy conserving membranes is suggested. (1) Padan E. and Rottenberg H. (1973) Europ. J. Biochem. 40, 431.

W-AM-E5 THE STRUCTURE OF THE CYTOCHROME a_3-Cu_A COUPLE IN CYTOCHROME c OXIDASE AS REVEALED BY NO BINDING STUDIES. T. Stevens*, G. Brudvig*, D. Bocian*, and S. Chan, California Institute of Technology, Pasadena, CA 91125.

There are two non-equivalent coppers in cytochrome c oxidase, only one of which is EPR visible. The EPR "invisible" copper is known to be antiferromagnetically coupled to cytochrome a_3 in the oxidized protein. In this work we have studied the interaction of NO with oxidized cytochrome c oxidase. Different results have been obtained depending on whether NO interacts with the protein in the absence or presence of azide. In the absence of azide, we have obtained evidence for a ferricytochrome a_3, Cu(II)-NO complex. In the presence of azide, the observations suggest that a bridged ferrocytochrome a_3-NO-Cu(II) complex is formed. In both complexes, the antiferromagnetic coupling between ferricytochrome a_3 and the "invisible" copper observed in the native protein is broken. In addition, we have observed EPR signals attributable to ferricytochrome a_3 in the ferricytochrome a_3, Cu(II)-NO complex, and to the "invisible" copper in the cytochrome a_3-NO-Cu(II) complex. The relevance of these results to the structure of the cytochrome a_3-NO-Cu(II) complex.

W-AM-E6 RESONANCE RAMAN SPECTRA OF CYTOCHROME c OXIDASE. EXCITATION IN THE 600 nm REGION. D. Bocian,* G. Brudvig,* and S. Chan (Intr. by M. Raftery), California Institute of Technology, Pasadena, CA 91125, and A. Lemley,* and N. Petersen,* Cornell University, Ithaca, N. Y. 14853.

Resonance Raman spectra have been obtained of oxidized and reduced cytochrome c oxidase with excitation at several wavelengths in the 600 nm region. No evidence was found for laser-induced photoreduction of the oxidized protein with irradiation at $\lambda \sim 600$ nm, in contrast to the predominance of this process upon irradiation in the Soret region. Comparison of the Raman spectra of the oxidized and reduced protein indicates that there are no bands which can be attributed to copper-ligand vibrations. On the basis of excitation profiles, absorption spectra have been simulated for the two cytochromes in the protein species studied.

W-AM-E7 PLANT PEPTIDOGLUCANS AFFECT NITROGENASE ACTIVITY AND OXIDATIVE PHOSPHORLYLATION IN RHIZOBIUM TRIFOLII STRAIN T1. M. Skotnicki,* B. Rolfe,* and M. Reporter. Charles F. Kettering Research Laboratory, Yellow Springs, Ohio 45387 and Department of Genetics, Australian National University, Canberra, A.C.T., Australia.

Peptidoglucans can be obtained from the medium of plant cells cultured with rhizobia separated from the plant cells by bacterial filters. In cultures of the fast-grower R. trifolii strain T1, these peptidoglucans alone can induce nitrogenase activity (C_2H_2 reduction and H_2 production) and increase O_2 consumption. In protoplasts of strain T1, oxidative phosphorylation is increased by the peptidoglucans (O_2 consumption by 20% and ATP synthesis by 50%). The peptidoglucans function at levels of nanograms per ml, and do not merely act as substrates. Uncoupled mutants of strain T1 defective in Mg^{++}-ATPase activity and unaffected by m-CCCP have been isolated. These mutants are unaffected by the peptidoglucans.

W-AM-E8 MASS ACTION RATIOS FOR MITOCHONDRIAL CREATINE KINASE IN HEART: EVIDENCE FOR COMPARTMENTALIZATION. R. DeFuria*, M. Dygert*, E. T. Fossel, and J. S. Ingwall, Biophysical Laboratory and Dept. of Medicine, Harvard Medical School, Boston, MA 02115.

Creatine kinase (CK) activity has been found to be associated with various organelles in heart and skeletal muscle; in particular with mitochondria and myofibrils. A special significance has been ascribed to mitochondrial CK in terms of its functional association with the ATP-ADP translocase (Saks, et al., Arch. Biochem. Biophys. 173, 34, 1976). A model has been postulated for the flow of high-energy phosphate current from mitochondria to myofibrils in which CK and translocase interact, creating a local compartment for the CK substrates and products. Therefore, the end product of respiration becomes creatine phosphate (CrP) rather than ATP. An important early result which supported this model was that CrP synthesis by isolated mitochondrial preparations was inhibited by oligomycin, even in the presence of exogenous ATP. More recent studies (Altschuld and Brierly, J. Molec. and Cell. Cardiol. 9, 875, 1977) have suggested that simple mass action considerations are sufficient to explain these earlier results, thus eliminating the need to argue for a "compartmentation role" for the mitochondrial CK. We have verified that simple mass action considerations are important since we find that upon the addition of oligomycin to mitochondria prepared from rabbit heart, there is an increase in ADP concentration (0.02 to 0.08 mM) which accompanies the decrease in the rate of CrP synthesis (from +0.06 to -0.005 μmoles/min/mg protein). However, we have also found that such a preparation is capable of net CrP synthesis (+0.06 μmoles/min/mg protein) when the apparent mass action ratio (0.09) for the substrates and products of the CK conversion is greater than the apparent equilibrium constant for this conversion (0.01). Thus in an isolated mitochondrial preparation, we find evidence for a mitochondrial CK compartment.

W-AM-E9 31-P NUCLEAR MAGNETIC RESONANCE (NMR) STUDIES OF ISCHEMIA IN ISOLATED PERFUSED RAT BRAIN AT 37°C AND AT 20°C. W.I. Norwood,* C.R. Norwood,*, J.S.Ingwall, and E.T.Fossel* (Intr. by R.T. Ingwall), Harvard Medical School, Boston, Mass. 02115.

We have developed an isolated perfused brain model in order to study high-energy phosphate metabolism in brain. Neonatal Sprague-Dawley rats were cannulated and perfused through the ascending aorta. Soft tissues surrounding the calvarium, and cervical and thoracic spine were excised. This preparation, perfused with Krebs-Henseleit buffer was positioned in a 15 mm OD nmr tube for study. 31-P nmr spectra were obtained at 109.3 MHz, each requiring the averaging of 200-400 free induction decays. The 31-P spectra of well perfused brain show six major resonances representing the three phosphates of ATP, sugar phosphates, inorganic phosphate (P_i) and creatine phosphate (CrP). Preparations were equilibrated to 37°C or 20°C and following a control period were subjected to 20 minutes of ischemia followed by 15-20 minutes of reperfusion. Levels of CrP and ATP fell coordinately to 13±1% and 28±4% of control levels respectively by 15 minutes of ischemia at 37°C. This is distinctly different from rat heart where a fall in CrP significantly preceeds the fall in ATP induced by ischemia. At 20°C CrP fell rapidly in the ischemic perfused brain, while ATP remained unchanged. On reflow at 37°C, ATP and CrP recovered substantially, but failed to return to control levels. (51±16% and 52±8% respectively) Reflow returned the CrP levels to control value in the brains made ischemic at 20°C within 10 minutes of reperfusion. This study suggests that permanent changes in ATP and CrP pools induced by 20 minutes of normothermic (37°C) ischemia are attenuated by imposition of hypothermia (20°C) as a protective intervention.

W-AM-E10 ROLE OF THE ADP-ATP CARRIER IN MITOCHONDRIAL RESPIRATORY CONTROL. John J. Lemasters and Arthur E. Sowers, Dept. of Anatomy, Univ. of North Carolina, Chapel Hill, N.C. 27514

The importance of adenine nucleotide translocation on respiratory control during oxidative phosphorylation was evaluated in rat liver mitochondria. ATP production and oxygen consumption were measured as a function of atractyloside and phosphate (Pi) concentration. A ligand conservation plot relating atractyloside concentration and fractional inhibition of ATP production is linear and indicates that inhibition is proportional to the fraction of ADP-ATP carrier sites bound with atractyloside. Mitochondrial respiration coupled to active oxidative phosphorylation is proportional to log [Pi]. In the presence of partially inhibitory atractyloside, adenine nucleotide translocation must be rate limiting in the overall reaction of oxidative phosphorylation. Under these conditions Pi retains its influence on respiratory rate. Therefore, respiratory dependence on phosphate does not imply that adenine nucleotide translocation cannot be rate limiting in oxidative phosphorylation. Plots of atractyloside versus respiratory rate at different Pi are similar in shape. There is no increase in sigmoidicity with decreasing Pi that would suggest that the carrier is losing any rate limiting character as the rate of the reaction falls. In the presence of glucose and ATP, respiration is linearly proportional to hexokinase at concentrations below 400 U/g mitochondrial protein. Atractyloside inhibition curves become increasingly sigmoidal as hexokinase falls below 400 U/g protein. This finding demonstrates that when the carrier is not rate limiting, significant amounts of atractyloside can bind without producing a corresponding decrease in ATP production. It is concluded that adenine nucleotide translocation is rate limiting in the overall reaction of oxidative phosphorylation and is responsible for the phenomenon of respiratory control. Supported by NSF Grant PCM 77-20689 and the North Carolina Heart Association.

W-AM-E11 COUPLING FACTOR B IS A COMPONENT OF THE MITOCHONDRIAL P_i-ATP EXCHANGE SYSTEM. S. Joshi,* J. B. Hughes,* and D. R. Sanadi. Boston Biomedical Research Institute, Boston, MA 02114.

The ATPase complex (C1) made from ETPH by extraction with lysolecthin and subsequent zonal centrifugation in a sucrose gradiant yields a preparation with the highest reported P_i-ATP exchange activity (1,100 nmoles x min^{-1} x mg^{-1}) and thus contains all components required for energy transduction. It shows 12 to 14 bands in SDS-PAGE. If Factor B were a component of the enzyme system, its presence could not be readily detected in SDS gels since it is stained very poorly by dyes and its concentration by weight would be relatively low owing to its low molecular weight (15,000). Presence of Factor B is shown by the observation that C1 forms a distinct Ouchterlony precipitin line with anti-Factor B. A similar complex (C2) made from Factor B-depleted AE-particles forms no line and shows 3- to 4-fold stimulation of exchange activity by added Factor B. When the C1 is extracted with 3.5M NaBr to separate the membrane proteins (MP) from F_1 subunits, Factor B is detected by immunodiffusion in the soluble extract. MP made from C1 requires F_1 and shows partial dependence on Factor B for P_i-ATP exchange activity. MP made from C2 has very low exchange activity with only F_1. Addition of Factor B enhances exchange 10- to 15-fold and inhibits ATPase partially. F_1 and Factor B bind independently to MP, the latter in amounts far exceeding that necessary to saturate the activity. The results further indicate (ACS Abst. Sept. 1978) that Factor B is a part of the energy transducing P_i-ATP exchange system but is not necessary for ATPase activity.

W-AM-E12 THE USE OF Fe(II) TO STUDY THE REACTION MECHANISM OF $(Na^+{+}K^+)$ATPASE. Marjory Myers, P.J. Ouseph*, Marie Cassidy, and Adil E. Shamoo. University of Rochester, School of Med.& Dent., Rochester, NY 14642; Dept. of Physics, University of Louisville, Louisville,KY 40208; Dept. of Physiology, George Washington University Medical Center, Washington, D.C. 20005.

Microsomes rich in $(Na^+{+}K^+)$ ATPase activity were isolated by the method of Albers, et al. (PNAS 50:474, 1963) from Electrophorus electricus electric organ and further purified by the method of Kuriki and Racker (Biochem. 15:4951, 1976). ATPase activity, as assayed by the release of ^{32}P from γ-labeled ATP under optimal conditions for Mg^{2+}, Na^+, and K^+, was found to be inhibited by the addition of ferrous ion at concentrations greater than 0.05 mM. Ferric ion was ineffective as an inhibitor when compared to the ferrous form. Addition of increasing concentrations of Mg^{2+} partially reversed the inhibition. When ATPase activity was measured with optimal concentrations of Na^+ and K^+, varying Fe(II), and with no Mg^{2+} present, the ferrous ion was found to stimulate a ouabain sensitive activity at a concentration range of 0.1 to 1 mM. The maximal stimulation amounted to approximately 15% of the enzyme specific activity with Mg^{2+}, Na^+, and K^+. Fe(II) alone stimulated the Na dependent phosphorylation of the $(Na^+{+}K^+)$ATPase as measured by the incorporation of ^{32}P from γ-labeled ATP. Increasing Fe(II) concentrations also increased the level of phosphorylated intermediate in the presence of Mg^{2+} and Na^+. By these and other kinetic and intermediary experiments we will show that Fe(II) can substitute for Mg^{2+} in the ATPase reaction sequence. Preliminary data using ferrous ^{57}Fe as a Mössbauer probe will be presented.

This research is supported in part by U.S. DOE contract and has been assigned Report No. UR-3490-1502

W-AM-E13 THE Ca^{2+}-INDUCED TRANSITION IN MITOCHONDRIA. R. A. Haworth and D. R. Hunter, Institute for Enzyme Research, Madison, Wis. 53706.

It was shown previously that isolated mitochondria incubated at 30° undergo a Ca^{2+}-dependent reversible transition in permeability, configuration and function (Hunter, D. R., Haworth, R. A. and Southard, J. H. (1976) *J. Biol. Chem. 251*, 5069-5077). We now have evidence that the action of Ca^{2+} is exerted through binding at a transmembrane hydrophilic channel, an action which is itself specifically controlled by nucleotides and other ions. The permeability of mitochondria which have undergone the Ca^{2+}-induced transition can be modulated over a wide range simply by adjusting the concentration of free Ca^{2+} in the medium. In the presence of Ca^{2+}, both neutral and charged molecules of molecular weight <1000 pass readily through the membrane. The effect varies sigmoidally with respect to Ca^{2+} concentration, with an apparent K_m of 16 μM at pH 7.0. It appears likely that the trigger site is also the site for high affinity Ca^{2+} uptake. Added ADP, NADH and Mg^{2+} inhibit the Ca^{2+}-induced permeability. Mg^{2+} and other ions, including H^+, act like competetive inhibitors; ADP and NADH act like mixed-type inhibitors. NADPH relieves the inhibition by NADH. Electron microscopy shows that the permeability induced in these mitochondria by Ca^{2+} is still transitional in nature. It is concluded that mitochondria, whether or not they have previously undergone a transition, behave as though they individually have a certain probability per unit time of undergoing a transition to the permeable state, for any fixed concentration of Ca^{2+} and inhibitors. The reversibility, specificity and control of this effect of Ca^{2+} argues strongly for an important physiological role of the Ca^{2+}-induced transition.

W-AM-E14 AN ELECTROGENIC LOW MOLECULAR WEIGHT CALCIUM CARRIER FROM CALF HEART INNER MITOCHONDRIAL MEMBRANE. Arco Y. Jeng and Adil E. Shamoo. University of Rochester, School of Med. & Dent., Rochester, NY 14642.

A 3,000 dalton protein has been isolated from calf heart inner mitochondrial membrane based on the relative binding properties of Ca^{2+}, Mn^{2+}, and Mg^{2+} to the protein (Jeng, et al. (1978) PNAS-USA 75:2125). By phosphorus determination, 150 moles of phospholipid copurify with one mole of protein. The phospholipid content has now been reduced to less than 0.2 mole per mole of protein by using Sephadex LH-20 column chromatography. Before the delipidation procedure, the extraction of Ca^{2+} into the organic phase by the protein was not affected by the presence of picric acid, a lipophilic anion. These experiments may suggest either that the protein is nonelectrogenic (i.e. Ca^{2+}-protein complex is neutral), or that phospholipids may act as lipophilic anions. After delipidation, picric acid is absolutely required for the protein-mediated extraction of Ca^{2+} into the organic phase (Shamoo, et al. in Frontiers of Biological Energetics:From Electrons to Tissues, Scarpa et al., eds. Academic Press, 1978). Picric acid also enhances the protein-mediated Ca^{2+} translocation between two aqueous phases separated by a bulk organic phase. The selectivity of the protein for divalent cations remains the same before and after delipidation. The relative sequence is Ca^{2+}, Sr^{2+} > Mn^{2+} > Mg^{2+}. The significance of this protein in the mitochondrial Ca^{2+} transport system will be discussed.

This research is supported by U.S. DOE contract and is assigned Report No. UR-3490-1503.

W-AM-E15 TOPOGRAPHICAL LOCATION OF CYTOCHROMES *b* ON EACH FACE OF THE INNER MITOCHONDRIAL MEMBRANE. H. James Harmon and P. F. Basile*, School of Biological Sciences, Oklahoma State University, Stillwater, OK 74074.

The surfaces of intact beef heart mitochondria and electron transport particles (ETP) of opposite orientation were cross-linked with exogenous proteins in an attempt to locate cytochromes *b*. Partially purified "cytochrome oxidase fraction" isolated by deoxycholate solubilization of mitochondria was cross-linked to intact mitochondria and ETP using copper-orthophenanthroline (CuOP) to catalyze the formation of covalent disulfide bridges. Following cross-linking, the membranes were treated with 1 M KCl and deoxycholate at a level such that cytochrome oxidase fraction sediments upon centrifugation and cytochromes *b*, *c*, and c_1 remain in the supernatant. If cross-linking occurs between exogenous oxidase and membrane-bound cytochrome *b* cross-linked samples should contain larger amounts of cytochrome *b* than control samples. Since CuOP is impermeant to the membrane, if linking occurs, the 2 proteins must be exposed to the medium. In both ETP and intact mitochondria (each with greater than 90% of the vesicles possessing the desired orientation) significantly greater amounts of cytochrome *b* appear in the cytochrome oxidase fraction following solubilization and centrifugation of the linked membranes. A 4- to 7-fold increase in cytochrome *b* content in the pellet is observed. If exogenous "cytochrome oxidase fraction" is not present during cross-linking or if Cu++ is not present during linking, differences in cytochrome *b* distribution are not observed. Differences in distribution of cytochromes *c* and c_1 are not observed. This suggests that cytochrome *b* is exposed on each membrane face.

W-AM-E16 pH-DEPENDENCE OF MITOCHONDRIAL K^+ FLUX. Joyce J. Diwan and David Aronson*, Biology Department, Rensselaer Polytechnic Institute, Troy, New York 12181.

Observations that unidirectional fluxes of K^+ both into and out of rat liver mitochondria are dependent on metabolic energy have been found to be inconsistent with the possibility that K^+ distributes passively across the mitochondrial membrane in equilibrium with a metabolism-dependent membrane potential (Diwan & Tedeschi, FEBS Lett. 60:176,1975). It has been suggested that the energy-dependence of K^+ influx and efflux may be explained on the basis of two passive mechanisms, a K^+ uniport mediating electrophoretic K^+ entry and a K^+/H^+ antiport mediating K^+ efflux (Chavez, Jung & Brierley, Arch. Biochem. Biophys. 183:460,1977). Unidirectional K^+ fluxes have been measured in rat liver mitochondria, in the presence of the respiratory substrate succinate, by means of the radioisotope ^{42}K. Some experiments have been carried out in the presence of N-ethyl maleimide (NEM), which blocks P_i/OH^- exchange, thereby preventing dissipation of experimentally manipulated pH gradients. Rates of K^+ influx and efflux are increased when the pH of the medium is increased from 7 to 8, in the presence or absence of NEM. In the presence of NEM, a linear dependence of K^+ influx on external OH^- concentration is observed at each of 4 K^+concentrations tested, from 1-13 mM. From the same data, Lineweaver-Burk plots of $1/(K^+$ influx) vs the reciprocal of the external K^+ concentration, at 4 pH values from 6.8-8.0, intersect to the left of the vertical axis. The same conditions that stimulate K^+ influx, increased pH and increased K^+ concentration in the medium, stimulate K^+ efflux. These results do not support the proposal that K^+ efflux occurs via a passive K^+/H^+ antiport. The dependence of K^+ influx on external pH and K^+ concentration is consistent with the proposal (Diwan & Lehrer, Membrane Biochem. 1:43,1978) that a sequential reaction mechanism is involved in energy-linked transport of K^+ with OH^- into the mitochondria. Supported by NIGMS Grant GM-20726.

W-AM-E17 CYTOCHROME C OXIDASE: AN ELECTRONIC $\Delta\tilde{\mu}H^+$ GENERATOR.
S.Papa, F.Guerrieri+, M.Lorusso+, D.Boffoli+, and F.Capuano+. Institute of Biological Chemistry, Faculty of Medicine, University of Bari, Italy.

The mechanism of $\Delta\tilde{\mu}H^+$ generation by cytochrome c oxidase was studied by analysis of H^+ transfer associated to oxidation of terminal redox carriers or exogenous reductants. Flow analysis in mitochondria and submitochondrial particles showed that H^+consumed for reduction of oxygen to H_2O reach the oxidase from the inner side of the membrane. Oxidation of cyt.c and cyt.a a_3 was not accompanied by transmembrane H^+ translocation. An H^+release at the outer side of the membrane, observed in this transition, was due to antimycin-insensitive redox events in the UQ-cyt.c span. It is demonstrated that the aerobic oxidation of ferrocyanide or exogenous ferrocyt.c by mitochondria caused no H^+ translocation but that arising from consumption of H^+ from the inner aqueous phase for reduction of oxygen to H_2O. This situation can, however, be complicated by H^+ release at the outer surface of the membrane caused by reactions unrelated to the function of cytochrome oxidase. It is shown that with ferrocyanide H^+ release was caused by antimycin-insensitive redox-reactions elicited by ferrocyanide/ferricyanide in the UQ-cyt.c span. The transition of exogenous ferrocyt.c to the ferric state caused artifactual scalar H^+ release from the outer surface of the membrane. This invalidates evidence produced by Wikström (1977) for existence of a H^+ pump in cytochrome c oxidase. The results presented provide, on the other hand, compelling evidence that cytochrome oxidase generates transmembrane $\Delta\tilde{\mu}H^+$ by vectorial electron flow from cyt.c at the outer side of the membrane to H^+ from the inner aqueous phase (Mitchell,1966,1978;Papa et al.1974,1978).

W-AM-F1 STIMULATION OF SERUM CHOLINESTERASE ACTIVITY BY CAFFEINE.
H.K. O'Farrell*, H.D. Brown, S.K. Chattopadhyay, and Y.T. Das*, NJAES, Rutgers University New Brunswick, N.J. 08903

Reaction rate between human serum cholinesterase and acetylcholine chloride was measured after incubating the serum with varying amounts of caffeine, viz., 2.15, 5.48 and 12.38 mg/ml serum. Incubation was carried out for 15 min with appropriate amounts of caffeine in 40% serum in 0.1 M Tris-HCl buffer (pH 8.0) at 25°C. Acetylcholine chloride was used @5.5 x 10^{-6} mole/ml serum in a total reaction mixture of 2.0 ml. Evaluation was based on the ballistic response of the reaction carried out in a Tian-Calvet type microcalorimeter. We found that the lower dose of 2.15 mg/ml enhanced the enzyme activity by 14.3% compared with caffeine-free serum activity, while the higher dosages of 5.48 and 12.83 mg/ml were inhibitory. We tested this stimulatory effect by 2 other standard methods of cholinesterase assay using 1 mg caffeine/ml serum for a spectrophotometric method (incubated in 50% serum in 0.1 M sodium phosphate buffer, pH7.8; acetylcholine chloride @8.5 x 10^{-4} mole/ml serum in a total reaction mixture of 5.6 ml), and 6.67 mg/ml for a pH-stat method (incubated in 4% serum in saline; pH maintained at 8.0; acetylcholine chloride @3.7 x 10^{-4} mole/ml serum in a total reaction mixture of 9.6 ml). The enzyme activity was found to be increased by 13.4% in the spectrophotometric assay and 6.3% in the pH-stat assay. A stimulatory dose of 2.15 mg/ml serum would translate itself to 6.5 g/individual-- a dosage that approaches toxic level for an average individual. The reaction kinetics of serum cholinesterase as well as acetylcholinesterase in the presence of caffeine are being further studied to shed light on the diverse pharmacological actions of caffeine.

Supported by USPHS grant GM22679 and Hatch NJ 00915.

W-AM-F2 A SPIN LABEL ASSAY FOR METAL COMPLEXATION.
Stephen Wagner*, A.D. Keith*, and W. Snipes (Intr. by Jeffrey Sands), The Pennsylvania State University, University Park, PA 16802.

Techniques for studying the complexation of metals with organic compounds include electrical conduction, x-ray diffraction, colorometric, gravimetric, and potentiometric analysis. These techniques are either not applicable or inconvenient for the study of biological systems due to narrow physiological pH ranges, lack of net orientation, turbidity and small sample size of most biological preparations. Development of a spin label assay for metal complexation based upon electron spin exchange between a paramagnetic ion and the spin label TEMPONE has provided a simple, rapid and sensitive method to study chelation in a diverse range of biological preparations. Chelators can: 1) form covalent-like bonds with the metal resulting in a reduction of the metal's magnetic moment, 2) reduce the concentration of free metal in solution, and 3) reduce the number of approaches by which the complexed metal and the spin label's electron wave functions can overlap. These effects result in a reduction of the spin label line-broadening caused by the paramagnetic ion. Linewidth changes resulting from pH titration and metal saturation studies may provide information regarding charge properties and metal-ligand stoichiometry of the molecular complexes. Competition studies of Ni^{++} and Zn^{++} for SDS micelles illustrate the plausibility of determining relative stability constants for systems where the configuration of the metal complex does not appreciably change with the addition of another cation. This work was supported by the U.S. Department of Energy.

W-AM-F3 "BIOCHEMICAL MAPPING" AN APPROACH TO DEFINING BODY COMPOSITION BY MEANS OF RADIOLABELED PHARMACEUTICALS.
Richard P. Spencer, Larry A. Spitznagle,* Parvathi Hosain,* Fazle Hosain.* Dept. Nuclear Medicine, Univ. Connecticut Health Center, Farmington, CT. 06032

Availability of specific pharmaceuticals, which carry an externally detectable label (gamma ray or positron), permits an approach to defining the location of body components during life, relatively noninvasively. There are at least 4 approaches. 1. Localization of transport events. An early example was use of radioiodide to study iodine transport by the thyroid. Initial distribution of Se-75-selenomethionine likely also measures an active transport system (the neutral amino acids). 2. Substrate utilization. This can be approached by means of a radiolabeled substrate or analogue (such as deoxyglucose with C-11 or F-18 radiolabels). If transport is not the limiting event, then movement intracellularly depends upon metabolism. Dual labels could be potentially employed to follow the fates of distinct parts of a substrate molecule. 3. Enzyme localization. A radiolabeled and firmly bound (high affinity) enzyme inhibitor would be the most logical choice. An example is 3-iodoaminopterin, an inhibitor of dihydrofolate reductase. The principles are: (a) Binding to the enzyme in vivo, (b) displacement ("flushing") by an even more firmly bound inhibitor, and (c) when possible, recovery of the original labeled compound to demonstrate that it is intact. In almost all cases, the radiolabeled compounds are at high specific activity and well below the saturation of transport or metabolic events. Uptake of radiolabel (R) is then given by: R = f.C.F., where f is the fractional extraction, C is the concentration in the blood stream and F is the flow to the area. 4. Component binding. Not only specific receptors, but several compounds can be labeled by "biochemical mapping." (Supported USPHS CA 17802, NIH).

W-AM-F4 A SIMPLE IMMUNOLOGY TEST, I. Giaever, General Electric Corporate Research and Development, P.O. Box 8, Schenectady, New York 12301

A new surface test for detecting antibodies in the 1 μg/ml range is described. Antigen is first adsorbed on a small area of a glass slide. The glass slide is then exposed to a solution suspected of containing antibodies. After a suitable time, the slide is removed, washed, dried and then sprayed lightly with plastic particles that stick to the protein layers on the glass. When the glass slide is subsequently exposed to a weak acid, the antigen-antibody bonds are cleaved. The antibodies, if present, will leave the surface removing some of the plastic particles. The final result is a clear spot that marks the region of earlier antibody adsorption.

W-AM-F5 PREDICTION AND OBSERVATION OF 1/f NOISE FROM A MODEL SYSTEM.† M. B. Weissman, Univ. of Ill., Urbana, IL 61801, R. A. Isaacson,* and G. Feher, U.C.S.D., La Jolla, CA 92093.

The spectral density S(f) of fluctuations in many systems, including nerve membranes and ionic solutions is inversely proportional to frequency. The origin of this "1/f" noise has been the subject of extensive speculations. We present here the theoretical justification and observation of "1/f" noise from a model system: In the presence of certain singularities in the fluctuation weighting function, a "1/f" transport noise is predicted for simple physical systems (M. B. Weissman, J. Appl. Phys. 48, 1705, 1977). We have produced such a (quasi)-singularity in the light intensity pattern by focusing incoming laser light with a cylindrical lens; the light intensity is thus inversely proportional to the distance from the focal line. The noise in the intensity of the light scattered off a flowing solution containing polystyrene beads is produced by statistical (thermodynamic) concentration fluctuations. The observed spectral density of the noise is close to the theoretically predicted "1/f" behavior (see Figure). The high and low frequency rolloff points are determined by the transit time of the beads through the smallest and largest dimensions of the traversed light path. Other beam patterns gave the predicted noise spectra, including a $(\sin \alpha\, f/\alpha f)^2$ spectral shape for flow past a slit, where α is a constant of the system.

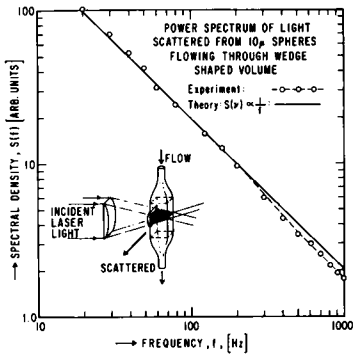

†Work supported by a grant from the NSF (DMR 77-14659).

W-AM-F6 TURBIDITY MEASUREMENTS IN AN ANALYTICAL ULTRACENTRIFUGE. GENERAL METHOD AND MASS-PER-LENGTH OF OPTICALLY ANISOTROPIC FILAMENTOUS VIRUSES. S.A. Berkowitz & L.A. Day. The Public Health Research Institute, New York, N.Y. 10016

Turbidity differences across sedimentation boundaries can be recorded with a conventional optical density (OD) scanner of an analytical ultracentrifuge, since $\Delta\tau = 2.303 \Delta OD$ per cm. Intense light at any of 334, 365, 405, 436 or 546 nm from source lamps containing Hg gives optimum scanner performance. Light of these wavelengths is suitable for light scattering studies on many biological macromolecules. Turbidity data extrapolated to zero concentration differences, Δc, yield $\Delta\tau/\Delta c = HMQ$, where H is the optical constant, M is molecular weight, and Q is a number that decreases from 1 toward 0 as dimensions and intraparticle interference effects increase. Dimensions and Q values can be obtained from the wavelength dependence of $\Delta\tau$. For long rods, Q becomes proportional to L^{-1} so that $\Delta\tau$ becomes a good measure of M/L if L is known. Appropriate expressions for Q must be used for anisotropic scatterers. The concentration differences across boundaries can be calculated from input concentrations and radial dilution, or can be measured by interference fringe displacements. Interference and scanner optics can be used simultaneously for the latter method, and also to obtain accurate dn/dc values. Results to date for fd, a filamentous virus 0.9μ length, give a value of dn/dc at 546 nm of 0.178 $g^{-1}cm^3$ and a mass-per-length of 18400 daltons/nm. Measurements have also been carried out on other viruses. Advantages of using an ultracentrifuge as a light scattering instrument are that, in runs of short duration, one or more macromolecular components can be characterized according to their sedimentation rates, dimensions, virial coefficients, and molecular weights. Also, sample volumes are small and are maintained dust free by the centrifugal field.

W-AM-F7 AN ANALYTICAL CENTRIFUGE DATA ACQUISITION SYSTEM UTILIZING PHOTON COUNTING TECHNIQUES AND A MINI-COMPUTER T.R. Tice*, L. Larkin,* and D. Higgins,* (Intr. by J. Lebowitz), Univ. of Alabama, Birmingham, Alabama 35294

A mini-computer assisted, data acquisition device utilizing photon counting techniques has been interfaced to a Beckman Model E analytical centrifuge. The device is inexpensive to construct (∿ $200 for components), contains pulse counting circuits, all timing circuits, cell accounting circuits and is capable of interrogating all six cell positions of an AN-G rotor during one rotor revolution at speeds of ≤ 40,000 rpm. Pulses taken directly from the scanning photomultiplier are amplified, discriminated, and shaped. Counting of these modified pulses occurs when either the sample or reference sector of each cell aligns with the incident beam and this is determined by adjustable timing circuits initiated by rotor collar signals. The pulse counting time interval is also variable and uses these timing circuits. The number of pulses counted per time increment is proportional to the light intensity. A record of sample and reference sector intensities verses radial distance for each cell is stored in memory for subsequent optical density and sedimentation calculations. A minor change to the scanning motor circuits gave computer control of the photomultiplier carriage. The system was tested by determining molecular weights of standard proteins using equilibrium ultracentrifugation techniques. Good molecular weights were obtained using as little as 5 μg of protein sample.

W-AM-F8 EVALUATION OF THE BECKMAN JE-6 ELUTRIATOR SYSTEM FOR THE FRACTIONATION OF CELLS AND PARTICLES INTO HOMOGENEOUS POPULATIONS. C.K.N. Li*, P.C. Keng*, S.A. Frank*, and K.T. Wheeler, University of Rochester Cancer Center, Rochester, N.Y. 14642.

In principle, centrifugal elutriation is a separation process in which particles are subjected to a centrifugal force balanced by an opposing force from a continuously flowing fluid surrounding the particles. Separation of the particles on the basis of their physical properties (volume, density, etc.) is then brought about by varying the rotor speed or the fluid flow velocity. Cultured 9L rat brain tumor cells or latex microspheres of mean diameter 9.8 μm or 19.0 μm were fractionated with the Beckman JE-6 elutriator system. The number of particles and their size distribution were determined in each fraction. The separation was evaluated by comparing several parameters, including recovery, elution losses during loading, homogeneity of size distributions, rate of removal during fractionation, and dependence of mean particle size on rotor speed and fluid velocity, with those expected under ideal physical conditions. By pumping dye through the separation chambers, it was further possible to visualize the role of fluid flow in the separation process. This evaluation was performed for both the regular separation chamber and the Sanderson separation chamber presently available for the JE-6 system. Both chambers deviated significantly from ideality in a way that limits their usefulness for fractionating homogeneous populations of cells or particles from heterogeneous populations.

W-AM-F9 RAPID VESICLE SEPARATION BY FILTRATION OR CENTRIFUGATION USING AGGREGATION WITH BASIC POLYPEPTIDES. R.N. Rosier,* T.E. Gunter, and K.K.Gunter, University of Rochester, Rochester, N.Y. 14642

Techniques for rapid aggregation of small vesicles made of natural biological membranes or of reconstituted phospholipid or phospholipid protein mixtures by addition of the basic polypeptides polylysine and protamine have been investigated. Millipore filtration or centrifugation may be used with these techniques to obtain rapid and complete separation of the vesicles from the suspending medium. At low polylysine to vesicle weight ratios, different parts of the polylysine molecule are likely to associate with different vesicles causing aggregation and causing the amount of aggregation to increase with polylysine concentration. At high values of the same ratio, on the other hand, polylysine bound to the surface of a vesicle inhibits binding of other polylysine molecules to more than one vesicle causing aggregation to decrease with polylysine concentration. With protamine the structure of the protein limits the surface covering and charge repulsion effects at high protamine concentration and makes this effect much smaller than with polylysine. Optimum aggregation rates are found at intermediate values of the basic protein to vesicle weight ratio for polylysine (around 50 μg/mg for red blood cell vesicles, sacoplasmic reticulum vesicles and submitochondrial particles, and around 100 μg/mg for phospholipid vesicles and cytochrome oxidase vesicles). The corresponding optimum rates for protamine induced vesicle aggregation takes place at intermediate and higher values of the same ratios (above 50 μg/mg for both classes of vesicle). Under ideal conditions the aggregation and filtration process can often be carried out in less than 15 or 20 seconds. Leakage induced by polylysine has been found to be troublesome at times when polylysine is used with phospholipid or cytochrome oxidase vesicles although not with vesicles made from natural membranes. Protamine aggregation was found to induce much less leakage than polylysine.

W-AM-F10 ELECTRON DIFFRACTION ANALYSIS IN PROTEIN CRYSTALLOGRAPHY. B. B. Chang and D. F. Parsons, Div. of Labs. & Res., N.Y. State Dept. of Health, Albany, NY 12201.

We have been investigating the possibility of using high-resolution electron-diffraction (ED) patterns from wet protein microcrystals for image reconstruction and crystallographic analysis. From the ED patterns, the unit-cell dimensions and space-groups of the protein crystals can be directly determined. Further structural information on the protein molecules requires analysis of the relative intensity of the diffracted beam in reciprocal space and obtaining the necessary phase information. Organic crystals with small unit cells and inorganic materials exhibit a significant dynamical effect due to coherent interaction of the multiply scattered beams. This makes structural analysis very difficult. Macromolecular crystal platelets give indications that the interaction with the electron beam may be nearly kinematical. Some of these indications include the absence of bending contours and the small relative intensities of all the diffracted beams compared to the incident beam. The intensities of the diffracted beams from kinematical scattering have been characterized by theory. Particularly, the relative intensity of a low-angle reflection is shown to increase as the square of crystal-thickness. ED patterns recorded by low-fluence technique are compared with the expected results from kinematical diffraction. The thickness of the wet crystals is measured with an interference microscope. The ED patterns are digitized with the computer-controlled Perkin-Elmer microdensitometer. User-interactive computer programs with PEP-terminal display have been developed to index the ED patterns to give background-corrected reflection intensity data. While phase information necessary for image reconstruction may be obtained from the isomorphous-replacement technique, improved phasing by the Gerchberg-Saxton interation procedure using medium-resolution images and high-resolution ED data is being tested. This work was supported by NSF Grant PGM 77-24212.

W-AM-F11 PERFORMANCE PARAMETERS OF IMAGE CONVERTERS FOR THE HIGH-VOLTAGE ELECTRON MICROSCOPE. Murray Vernon King and Donald F. Parsons, Electron Optics Laboratory, Division of Laboratories & Research, New York State Department of Health, Albany N. Y. 12201.

Attractive alternatives to photographic recording of images in the high-voltage electron microscope are offered by image converters of various types, including phosphor screens coupled to low-light-level television cameras via fiber optics or lenses, diode arrays and charge-coupled devices, and crossed wire-grid anodes. The advantages of these devices include greater yields of quantum events per incident 1-MeV electron than in photographic recording, with consequent diminution of quantum noise, and potentialities for direct input of images into computers for image processing. Performance of devices is rated experimentally by a computer program that we have developed for direct conversion of edge profiles to the modulation transfer function (MTF), together with measurement of dynamic noise, moiré distortions of images, etc. Theoretical estimates of performance are based on calculations of the effect on MTF of multiple scattering of electrons and light spread in phosphors. In particular, the multiple-scattering calculations show that the sensitive volume of any imaging detector for 1-MeV electrons must be restricted to a thin layer no more than about 200-μm thick, the limit depending on the working material and the allowable blur. This is why some otherwise attractive imaging devices such as microchannel plates offer little promise for applications in the high-voltage electron microscope. This work has been supported by grants RR-00754 and RR-01088 awarded by the Division of Research Resources of the National Institutes of Health, PHS/DHEW. Measurements have been made on the high-voltage electron microscopes of the New York State Department of Health (*Tonatiuh*) and of the University of Wisconsin.

W-AM-F12 QUANTITATION OF RADIATION DAMAGE TO BIOLOGICAL SPECIMENS INCURRED DURING EXAMINATION IN THE ELECTRON MICROSCOPE. Murray Vernon King and Donald F. Parsons, Electron Optics Laboratory, Division of Laboratories & Research, New York State Department of Health, Albany N. Y. 12201.

Radiation damage to biological specimens caused by the electron beam employed to examine them in the electron microscope is a serious factor that restricts the amount of information that can be obtained in this instrument. The situation is complicated in the high-voltage electron microscope by the variation of σ_i/σ_e with electron energy, and can become especially serious in this instrument unless special measures are taken to combat the need for lengthy exposures occasioned by the low stopping power of the recording materials for fast electrons. While embedded sections of cells and tissues have usually been regarded as relatively resistant to radiation damage, this proves true only of features utilized for qualitative recognition, such as the contours of membranes. Radiation damage to tissue sections can be traced by sequential exposures to chosen areas, with comparison of the images by a stereo-color technique and quantitative measurement of distortions. Progressive charring of the embedding plastic in the electron beam leads both to collapse of the specimen in the direction normal to the specimen plane and to smaller but considerable lateral distortions. In view of the increasing importance of techniques that require more than one micrograph taken from the same specimen area, such as stereo pairs and tilt series for 3D reconstruction, multiple micrographs either must be taken under low-fluence conditions that minimize radiation damage or allowance must be calculated for the distortions caused by it. This work has been supported by grants RR-00754 and RR-01088 awarded by the Division of Research Resources of the National Institutes of Health, PHS/DHEW.

W-AM-F13 ELECTRON DIFFRACTION OF CHRYSOTILE ASBESTOS BOMBARDED WITH 100 to 1000 keV ELECTRONS. A. J. Ratkowski*, B. B. Chang, and D. F. Parsons, Division of Laboratories and Research, New York State Department of Health, Empire State Plaza, Albany, NY 12201.

The pathogenic effects of high concentrations of airborne chrysotile asbestos are well established. Because these fibers in environmental samples tend to be extremely small (length <1 μm, diameter 20-50 nm), the only microanalytic technique suitable for identifying individual fibers is electron diffraction. However, there has been no systematic study reported which examines how the chrysotile electron diffraction pattern changes as the energy of the incident electrons is varied. To investigate this relationship, we have obtained electron diffraction patterns from such fibers bombarded with electrons at incident energies of 100 to 1000 keV in our high-voltage (1.2 MV) electron microscope at Albany, New York. Our results bear upon at least four factors in the electron diffraction process: (i) The influence of fiber size on the partition between dynamic and kinematic electron scattering. This factor has not been considered in earlier electron diffraction studies of chrysotile asbestos. (ii) Microdensitometric assessment of contrast in the diffraction patterns. (iii) The effect on the diffraction pattern of radiation damage induced by electron beams at varying doses from 100 to 1000 keV. (iv) The advantages of a double-tilt specimen holder capable of rotation through angles of ± 39° and ± 57° about two mutually-perpendicular tilt axes.

W-AM-Po1 LIPID-PROTEIN ASSOCIATIONS IN CHROMATOPHORES FROM THE PHOTOSYNTHETIC BACTERIUM RHODOPSEUDOMONAS SPHAEROIDES. G.B. Birrell*, W.R. Sistrom*, and O.H. Griffith, University of Oregon, Eugene, OR 97403.

Lipid-protein interactions were examined in chromatophores isolated from the photosynthetic bacterium Rhodopseudomonas sphaeroides using lipid spin labels. The chromatophores contain fluid bilayer and a significant amount of lipid immobilized by membrane proteins. For a typical preparation of cells grown under 600 ft-c illumination, 59% of the spin labeled fatty acids were bound. Essentially the entire length of the 18-carbon fatty acid chain was immobilized, judging from results obtained with the spin label at the 7, 12, and 16 positions. The amount immobilized varies directly with the bacteriochlorophyll content of the chromatophore material, suggesting that a significant fraction of the lipid spin labels is immobilized on the hydrophobic surfaces of the chlorophyll-binding proteins. Changing the lipid spin label head group from a negatively charged carboxyl group to a positively charged quaternary amine greatly decreased the amount of immobilized lipid. The changes in immobilized lipid with light level and polar head group suggest that the antenna bacteriochlorophyll-binding proteins preferentially associate with negatively charged lipids.

In addition several chlorophyll-derived spin labels have been prepared. The potential use of these labels to study specific chlorophyll-protein interactions and flip-flop will be discussed.

W-AM-Po2 DIFFUSION IN MEMBRANES: HOW MUCH DOES THE VISCOSITY OF THE AQUEOUS PHASE AFFECT DIFFUSION RATES OF MEMBRANE PROTEINS AND LIPIDS? C.L. Wey‡ R.A. Cone, Dept. of Biophysics, and B.J. Gaffney, Dept. of Chemistry,(Intr. by W. Love), Johns Hopkins University, Baltimore, MD 21218

We find that the relaxation time for rotational diffusion of bacteriorhodopsin in reconstituted DML (dimyristoylphosphatidylcholine) vesicles increases by about 50% when 30% (w/w) glycerol is added to the vesicle suspension. Similarly, we have previously reported that solutions with 30% (w/w) glycerol or 30% sucrose increase the rotational relaxation time for rhodopsin in intact disk membranes by about 100%. (Rhodopsin probably protrudes considerably more into the aqueous phase than does bacteriorhodopsin.) Using lipid phase spin probes, we find that 30% glycerol or sucrose solutions slow the motion of the probes in bacteriorhodopsin—DML vesicles and in intact disk membranes as follows: (1) With a probe small enough to tumble in the lipid phase (2,2,4,4-tetramethyl-1,2,3,4-tetrahydro-γ-carboline-3-oxyl: 5Åx8Å x11Å), the estimated correlation time increased about 30% in the vesicles,and 20% in intact disk membranes. (2) Spin probes attached to fatty acids at the 5th, 10th, or 16th carbon atoms from the carboxyl end (5-,10-,or 16-doxylstearic acid) showed changes in EPR spectra which could be matched by lowering the temperature by 3, 2, and 0°C, respectively. Decreases in temperature by these amounts slow the rotational relaxation times of rhodopsin and bacteriorhodopsin by about 20%,15%, and 0% respectively. The glycerol and sucrose solutions used in these experiments increased the aqueous phase viscosities by about 2.5x. Therefore, the increase in the effective viscosity experienced by the lipid phase spin probes appeared to increase on the order of 1/10 the increase in aqueous phase viscosity while the effective viscosity for rotational diffusion of proteins increased by about 1/3 the increase in aqueous phase viscosity. (Supported by NIH grant EY 00520 and CA 15997.)

W-AM-Po3 THERMODYNAMICS OF PROTEIN-LIPID INTERACTIONS. Ernesto Freire and Rodney L. Biltonen, Department of Biochemistry, Univ. of Virginia, Charlottesville, VA 22908.

Thermodynamic equations of the annulus model for protein-lipid interactions in biological membranes have been solved in terms of structural and thermodynamic parameters of the pure components. These derived equations provide a functional relation between the enthalpy and entropy changes of the gel-liquid crystalline transition and the protein:lipid ratio, thus prescribing simple ways of interpreting calorimetric data and testing the annulus model in terms of the various parameters of the system. In addition, possible changes in the state of aggregation of the protein molecules during the gel-liquid crystalline transition have been included into the model. It is shown that the physical state of the lipid bilayer and the in-plane distribution of protein molecules are correlated quantitatively. The biological implications of this correlation are discussed.

W-AM-Po4 MODULATION OF THE ACTIVITY OF MEMBRANE PROTEINS BY LIPID TRANSITIONS. Brian Snyder* and Ernesto Freire, Dept. of Biochem., Univ. of Virginia, Charlottesville, VA. 22908.

A simple cooperative model for the gel-liquid crystalline transition of the lipid bilayer has been used to investigate the correlations between the physical state of the bilayer matrix and the chemical potential of membrane proteins. It is shown that the state of aggregation of membrane proteins can be modulated by small changes in the physical state of the lipid bilayer and that the temperature at which the protein changes occur (T_p) does not necessarily coincide with the actual transition temperature (T_m) of the bilayer. The magnitude and the direction of the displacement (T_p-T_m) depends on the protein:lipid ratio and the difference between the protein-lipid interaction energies above and below the bilayer phase transition. These theoretical results offer a qualitative rationale for the experimental observation that ligand or enzyme activity curves and phase transition profiles are often separated from each other in the temperature scale.

W-AM-Po5 THEORETICAL MODEL OF PROTEIN-LIPID AND PROTEIN-PROTEIN INTERACTIONS IN BILAYER MEMBRANES. J. C. Owicki and H. M. McConnell, Dept. of Chemistry, Stanford Univ., Stanford, CA 94305.

We have previously described a model for the perturbation of the order of lipids near an intrinsic membrane protein, based on a variational technique and Landau-de Gennes theory, in the limit of infinite protein dilution.[1] This work is now extended to nonzero protein concentration, under the approximation that the proteins are on a hexagonal lattice. Estimates are made of the strength and spatial dependence of the lipid-mediated interaction between proteins. The implications for phase separation into protein-rich and protein-poor phases in the plane of the membrane are discussed. It is found that protein-lipid interactions exert strong effects on the phospholipid solid-fluid phase transition. In the presence of proteins, the thermal transition has a broad and a sharp component. With increasing protein concentration, the enthalpy change associated with the sharp transition decreases, and the temperature of the transition deviates increasingly from the transition temperature of the bulk phospholipid. It is intriguing that the model also qualitatively reproduces several experimental observations on the physical behavior of bilayers formed from mixtures of cholesterol and phosphatidyl cholines. The possible relevance of the theory for this system is discussed.

[1]J. C. Owicki, M. W. Springgate, and H. M. McConnell, Proc. Natl. Acad. Sci. USA 75, 1616-1619 (1978).

This research was supported by the National Science Foundation Grant 77-23586. J.C.O. is the recipient of an Institutional Research Fellowship under the National Institutes of Health Grant GM-07026.

W-AM-Po6 FLUORESCENCE ENERGY TRANSFER LOCALIZATION OF PROBES, LIPIDS AND PROTEIN IN SERUM LIPOPROTEINS L.A. Sklar, M.C. Doody*, A.M. Gotto, Jr.*, and H.J. Pownall, Division of Atherosclerosis and Lipoprotein Research, The Methodist Hospital and Baylor College of Medicine, Houston, Texas 77030

Several fluorescent chromophores have been localized in lipoproteins. The primary acceptor 5-(N-hexadecanoyl)aminofluorescein (HAF), can be quenched by aqueous iodide; taken together with binding measurements we conclude that the chromophore resides exclusively at the lipoprotein surface at pH 7.5. Energy transfer from cis or trans-parinaric acid (PnA) or 16-(9-anthroyloxy)palmitic acid donors to HAF acceptors is consistent withthe position of fatty acid probes in the LDL and VLDL surface. Methyl ester and cholesterol ester derivatives of PnA are considerably less efficient donors than PnA (fatty acid) to HAF, suggesting substantial localization of these non-polar lipids with the lipoprotein core. Several models can account for the observed transfer if both probe acyl chain orientation and surface/core distribution are considered. Energy transfer from diphenylhexatriene (DPH) suggests a 50 Å average penetration of DPH into LDL. We speculate that the insensitivity of DPH to the thermal reorganization of LDL cholesterol ester may result from residual disorder either of cholesterol ester acyl chains or the LDL core. Tryptophan residues in LDL ApoB are donors to several probes. Tentative results indicate two classes of tryptophan donors, one near the surface/core interface and the other buried within the protein or near the aqueous interface. Lipoprotein surface heterogeneity is under investigation. (Supported by USPHS HL-17269, HL-19459, and AHA 76-1026. L.A. Sklar is a fellow of the Helen Hay Whitney Foundation).

W-AM-Po7 MODELS FOR FLUORESCENCE ENERGY TRANSFER IN SERUM LIPOPROTEINS, LIPOPROTEIN COMPLEXES AND MEMBRANES M.C. Doody*, L.A. Sklar, H.J. Pownall, J.T. Sparrow, A.M. Gotto, Jr.*, and L.C. Smith, Baylor College of Medicine, Houston, Texas 77030

Fluorescence energy transfer efficiencies in spatially restricted systems depend on the transfer efficiencies (T) and the average number of acceptors (F) for multiple acceptor regions encompassing all points within the effective radius of energy transfer. The ensemble quantum yield is calculated as $Q = (1 - F_1T_1)(1 - F_2T_2)\ldots(1 - F_nT_n)$, the product of individual quantum yields from transfer to each of the acceptor regions. Geometrical manipulations have permitted adaptation of this flexible approach to systems where donor:acceptor interaction is restrained by variable steric perameters. The systems include energy transfer in solution, two-dimensional mono- and bilayer energy transfer from the periphery to the interior of unilamellar discs, and transfer from donors distributed within a sphere to surface acceptors. The latter requires fitting to multiple weighted exponentials; this manipulation greatly extends the applicability of the method. The effect of such factors as R_o, radial and geometrical restrictions on the approach of donors and acceptors, acceptor concentration and particle dimensions are considered, where relevant. Energy transfer from N(2-naphthyl)-23,24-dinor-5-cholen-22-amide-3β-ol to N dansyldimyristoylphosphatidylethanolamine (DansDMPE) in dimyristoyl phosphatidylcholine (DMPC) bilayers showed the sterol napthyl group to be 13 Å from the level of DansDMPE, about the distance expected from model building. Energy transfer to Dans DMPE from TRP in a synthetic lipid-binding peptide with a putative amphipathic α-helix places TRP 16 Å from DansDMPE. Since the dansyl group is at the level of the glycerol backbone, we conclude the peptide helix penetrates beyond the DMPC ester region. (Welch Q-343, USPHS HL-15648, HL-17269).

W-AM-Po8 STRUCTURE OF RABBIT CHOLESTERYL ESTER-RICH VERY LOW DENSITY LIPOPROTEINS (CER-VLDL). J.D. Morrisett, H.J. Pownall, R.I. Roth*, A.M. Gotto, and J.R. Patsch*, Baylor College of Medicine, The Methodist Hospital, Houston, Texas 77030.

CER-VLDL from the plasma of rabbits fed a 1% cholesterol diet for ≥8 days were obtained by ultracentrifugation at d 1.006 g/ml. Zonal ultracentrifugation indicated that CER-VLDL comprised >95% of the total plasma lipoproteins in the cholesterol-fed state and that this material consisted of at least 3 density subpopulations with mean flotation rates ($S_{f\ 1.063}$) of 50, 95 and >170. Gel filtration chromatography over Sepharose 2B-CL indicated at least 2 major size subpopulations with mean diameters of 1164 and 586 Å as determined by quasi-elastic light scattering. The larger (smaller) particle consisted of 12(6)% protein, 11(17)% phospholipid, 2(3)% cholesterol, 68(71)% cholesteryl ester (CE), 8(2)% triglyceride. At 37°, the fluidity of CER-VLDL was 50% of that of normal rabbit VLDL as judged by partitioning of the EPR probe, TEMPO. The partition coefficient increased abruptly between 42° and 48°. DSC thermograms of CER-VLDL revealed reversible endotherms at 41.5° and 47.5° which became more intense after thermal denaturation at 97°. We assign these endotherms to the smectic → cholesteric and cholesteric → isotropic phase transitions of the CE, principally cholesteryl oleate (43% of CE) which has known transitions at 42° and 47.5°. The presence of CER-VLDL as the dominant lipoproteins, their low fluidity at physiological body temperature, and their positive correlation with the development of atherosclerosis in rabbits suggests that the physical state of the CE in these lipoproteins may be the cause of their atherogenicity. (Supported by HL-14194-04 and AHA 78-1042).

W-AM-Po9 PREPARATION AND CHARACTERIZATION OF RECONSTITUTED G PROTEIN-LIPID VESICLES FROM VESICULAR STOMATITIS VIRUS. Bernice I. Feuer[#] and John Lenard, Dept. of Physiology and Biophysics, CMDNJ-Rutgers Medical School, Piscataway, N.J. 08854.

The single glycoprotein (G) of vesicular stomatitis virus (VSV) has been isolated in high yield by extraction of the purified virions with 0.05 M. octyl-β-D-glucoside (OG) in 0.01 M. phosphate buffer, pH 8.0. The extract contains 60-80% of viral phospholipids, and is essentially free of other viral proteins. The efficiency of extraction of G protein decreases with decreasing pH, although the efficiency of extraction is not affected. Dialysis to remove OG results in formation of G protein-lipid vesicles of 300-800 nm diameter with at least 80% of the G protein susceptible to externally added protease. Addition of increasing amounts of soybean phospholipid to the viral extract before dialysis resulted in vesicles of decreasing protein:lipid ratios, as indicated by decreases in buoyant density. The G protein-lipid vesicles were effective in eliciting specific anti-G antibodies that neutralized viral infectivity by up to 80%, as determined from a neutral red assay of cell viability measured 11 hours after infection. Supported by grants from NIH and NSF.

[#]Present address: Department of Chemistry, Drew University, Madison, N.J. 07940

W-AM-Pol0 CRITICAL MICELLE CONCENTRATION OF GANGLIOSIDES. M. L. Johnson, S. Formisano*, G. Lee*, S. M. Aloj*, and H. Edelhoch*, CEB-NIAMDD-NIH, Bethesda, Md. 20014.

The monomer-micelle equilibria of mixed bovine gangliosides and purified G_{M1} were studied by equilibrium dialysis, gel filtration, band and boundary centrifugation in sucrose gradients. The dissociation of micelles is very slow (days) in water and thus equilibrium was approached by association of monomers rather than the dissociation of micelles. Consequently, the gangliosides were first converted into very low molecular weight aggregates (1-3 molecules) by dissolving in DMSO and then diluted into aqueous buffer. The mixed gangliosides revealed a slow equilibrium between two micellar sizes (i.e., 10 S and 4.5 S). The critical micelle concentration of the mixed gangliosides was found to be approximately 10^{-8} M by gel filtration, equilibrium dialysis and band centrifugation. G_{M1} was studied using the boundary centrifugation technique. This gave a sedimenting micelle of approximately 6.5 S and a non-sedimenting monomer concentration of 1-2 x 10^{-10} M (or less) which corresponds to the critical micelle concentration.

W-AM-Pol1 DEVELOPMENTAL DIFFERENCES IN PROTEOGLYCAN AGGREGATE FORMATION. A. G. Beaudoin and D. D. Dziewiatkowski,* (Intr. by R. Zand), Dept. of Oral Biology and DRI, University of Michigan, Ann Arbor, MI 48109.

The ground substance of cartilage contains an aggregating complex of proteoglycan subunits, hyaluronic acid and a protein "link." A progressive increase has been observed in the relative percentage of aggregate formed in preparations isolated from the cartilages of sheep at different stages of development (100 d. and 140 d. fetus, adult ewe). Polyacrylamide and SDS polyacrylamide gel electrophoresis demonstrate the presence of the link protein fraction. Analysis in the analytical ultracentrifuge has been performed upon constant weight fraction mixtures of the isolated proteoglycan subunit (A_1D_1) fraction, isolated link protein (A_1D_5) fraction and hyaluronic acid purified from rooster comb. Cross-reactive matching demonstrates that the A_1D_5 fractions of both fetal and adult preparations are functional. The A_1D_1 fractions isolated from fetal preparations, however, demonstrate a marked decrease in the ability to form aggregates. It is anticipated that work currently in progress will help to explain the apparent differences which exist in the binding region of the proteoglycan subunit.

W-AM-Pol2 SYNTHESIS AND CHARACTERIZATION OF INSOLUBLE CHONDROITIN SULFATE HYDROGELS. Edgar N. Jaynes, Jr* and Randall V. Sparer* (Intr. by S.P. Rao), Case Western Reserve Univ., Cleveland, Ohio 44106.

In an effort to prepare materials with a predicted low level of thrombogenic and immunogenic activity, chondroitin sulfate (CS), a glycosaminoglycan from connective tissue which is predominantly an alternating copolymer of N-acetyl-D-galactosamine-4-sulfate and D-glucuronic acid, has been crosslinked to form water-insoluble hydrogels. The glucuronic acid carboxyl group is reacted with S-protected cysteine methyl ester to form a peptide bond. The resulting compound is crosslinked by removal of the protecting group followed by formation of disulfide bonds using mild oxidants. The crosslinking reaction proceeds quickly to a stable product, but can be reversed by the addition of a reducing agent such as dithiothreitol. A range of gels resulting from the attachment of varying amounts of cysteine to CS has been investigated. Analysis of the product was accomplished using spectrophotometric assays for sulfhydryl groups and uronic acid; Fourier transform infrared spectroscopy analysis of the types and numbers of carbonyls, sulfur-sulfur bonds, and sulfur-hydrogen bonds present; and measurement of swelling parameters to determine the effective number of crosslinks formed. The use of this material as an implantable reservoir for controlled drug release will be described. The advantages of the use of biological molecules as opposed to materials not normally found in the body will be discussed.

W-AM-Po13 TRANSPORT PHENOMENA IN COLLAGEN GELS, M.L. Shaw and A.L. Schy*, Medicine/ Physiology and Biophysics, University of Washington, Seattle, Wa., 98195.

We measured by elution the partition coefficients (K_{av}) of various nonbinding tracers in 1%, 5%, and 10% gel columns ("bead" size 250-500 μm) formed from solubilized, purified, and subsequently recross-linked and granulated collagen. The fit of the partition coefficient data(K_{av} vs Stokes radius of tracer) with the Ogston-Laurent-Killander model was examined (A. G. Ogston, Trans. Faraday Soc. 54:1754, 1958; T.C. Laurent and J. Killander, J. Chromatog. 14:317, 1964). The calculated values for the gel parameters L (cm of fiber / cm^3 of gel phase) and r_r (effective fiber diameter) of this model are 5.1± 1.0, 7.2± 1.4, and 7.2± 2.2 for L (cm^{-2}) and 43.3± 10.8 for r_r (A°) for the 1%, 5%, and 10% gel columns, respectively. The model thus does not provide an internally consistent description for the entire gel "family" as indicated by the negative value of r_r for the 1% column.

Diffusion coefficients (D) were obtained from the increase in variance of the tracer elution curves (assumed Gaussian) in a stop-flow experiment compared with that for the standard small-zone elution with no interruption of flow. Values of D/D_o (free aqueous diffusion coefficient) at 4°C in the 5% gel column include 0.83 (H_2O), 0.76 (glucose), and 0.69 (FITC-dextran 20) and agree with predicted values based on the Ogston model for the gel phase within the estimated range of experimental error, 10-20% (A.G. Ogston, B.N. Preston, J.D. Wells, Proc. R. Soc. Lond. A 333:297, 1973). Supported by NIH Grants GM-24990 and HL-19139-03 and Joint Center for Graduate Studies, Richland, Wa. 99352.

W-AM-Po14 NEAR-INFRARED ANALYSIS OF WATER-BIOPOLYMER INTERACTION UTILIZING A VARIABLE PATH CELL. D.L. VanderMeulen and N. Ressler, Pathology and Biological Chemistry, Univ. of Illinois Medical Center, Chicago, IL 60612.

A novel and convenient method is presented for studying water-biopolymer interaction, including direct empirical resolution of near-infrared difference spectra into "hydration" and "excluded volume" components. This technique utilizes a commercially available variable pathlength absorption cell, enabling spectral examination of aqueous solutions of proteins, nucleic acids, etc. without extraneous additions or alterations of the material under study. Time-dependent changes by the action of various proteolytic enzymes and ribonuclease upon appropriate substrates were followed. For example, with the action of subtilopeptidase on ovalbumin, the water absorbance in the 1.4-1.5 μm region progressively decreases as the solvent volume excluded by the system increases by digestion of the relatively compact globular substrate into fragments. In addition, there is a progressive increase in absorbance in the region just beyond ca. 1.5 μm, assigned to the increase in the hydrated water (which absorbs at lower energy compared to the bulk water that includes relatively non-bonded water). The wavelength maxima of the component curves resolved by the variable path analysis were in agreement with expectations based on relevant literature, for both the spectral components representing the relative hydration (1.49 μm) and excluded volume (1.45 μm). Additional information was obtained by studying the effects of pH, buffer, and heat or detergent denaturation.